arXiv:2312.16734v1 [stat.ME] 27 Dec 2023

Selective Inference for Sparse Graphs via Neighborhood Selection

Yiling Huang
Department of Statistics, University of Michigan
and
Snigdha Panigrahi*
Department of Statistics, University of Michigan
and
Walter Dempsey
Department of Biostatistics and Institute for Social Research,
University of Michigan

December 29, 2023

Abstract

Neighborhood selection is a widely used method used for estimating the support set of sparse precision matrices, which helps determine the conditional dependence structure in undirected graphical models. However, reporting only point estimates for the estimated graph can result in poor replicability without accompanying uncertainty estimates. In fields such as psychology, where the lack of replicability is a major concern, there is a growing need for methods that can address this issue.

In this paper, we focus on the Gaussian graphical model. We introduce a selective inference method to attach uncertainty estimates to the selected (nonzero) entries of the precision matrix and decide which of the estimated edges must be included in the graph. Our method provides an exact adjustment for the selection of edges, which when multiplied with the Wishart density of the random matrix, results in valid selective inferences. Through the use of externally added randomization variables, our adjustment is easy to compute, requiring us to calculate the probability of a selection event, that is equivalent to a few sign constraints and that decouples across the nodewise regressions. Through simulations and an application to a mobile health trial designed to study mental health, we demonstrate that our selective inference method results in higher power and improved estimation accuracy.

Keywords: Covariance selection, Gaussian graphical models, Network analysis, Penalized regression, Post-selection inference, Selective inference.

*The author acknowledges support by NSF grants 1951980 and 2113342.

1 Introduction

The network approach to psychopathology posits mental disorders can be conceptualized as systems of co-occurring symptoms (Cramer et al., 2012, 2010). From this perspective, symptoms are not indicators of a latent "common cause" but a complex network. Aiming to identify the inter-symptom relations, there has been a growing focus on methods for estimating conditional dependence relationships in undirected graphs. Such methods have provided psychologists with a useful tool for learning complex relationships between different variables. In psychology, these undirected graphs are often based on Gaussian graphical models (GGMs) (Epskamp et al., 2018b). Consider, for example, the *Providing Mental health Precision Treatment (PROMPT) Precision Health Study* which is a 12-month mobile health (mHealth) intervention trial focused on augmenting standard care to improve health outcomes by using mobile health technologies to extend the reach outside the clinic. A key scientific aim of PROMPT is to better understand the relationships among treatment, baseline demographic information, survey responses, and mobile health signals.

A common concern with network analysis in psychology is replicability (Maxwell et al., 2015; Fried and Cramer, 2017; Forbes et al., 2019). Some have commented on the instability of network methods (Borsboom et al., 2017), while others have argued the instability is caused by the use of single-item assessments and small samples (DeYoung and Krueger, 2018). To promote robustness, methods have been developed for evaluating the precision and stability of estimated parameters (Epskamp et al., 2018a). In this paper, we identify and address one such relevant cause, called a silent killer of replicability (Benjamini, 2020), when selection bias from the estimated conditional dependence relationships in graphical models is simply ignored during inference. Several methods have been adopted in the empirical network literature to estimate conditional dependence relationships and attach

point estimates to such relationships. Nonetheless, the issue of replicability is still a subject of ongoing debate (Forbes et al., 2019), especially because psychology continues to grapple with a replication crisis, as noted by Maxwell et al. (2015).

While modeling the conditional dependence relationships in multivariate mHealth data is an indispensable goal, given the risk of false discoveries and growing concerns of replicability, reporting findings from the estimated graph can be grossly misleading without accompanying uncertainty estimates for the matched parameters. Recognized as a problem of "post-selection inference" or "selective inference" (Benjamini and Yekutieli, 2005; Berk et al., 2013a; Lee et al., 2016b), countering selection bias from the estimation of such conditional dependence relationships remains a key, unaddressed challenge.

In this paper, we propose a selective inference approach to quantifying the uncertainty in the estimated graph for mHealth data. Our focus is on the Gaussian graphical model, which associates an undirected graph to p jointly normally distributed random variables. The nodes of the graph represent these variables, while the edges between the nodes capture their conditional dependence relationships. These relationships are characterized by the nonzero entries of the inverse covariance matrix, also known as the precision matrix. In short, we will refer to this model as GGM and provide a brief overview of it in the next section.

The rest of our paper is organized as follows. In Section 2, we review the GGM and the neighborhood selection approach, which is a multivariate regression method used for estimating conditional dependence relationships. In the same section, we discuss the contributions of our selective inference method. In Section 3, we present our method to address feasible selective inferences for the estimated edges in the GGM. We provide an efficient algorithm that can be used to numerically compute a pivot for selective inference, which

can produce p-values and confidence intervals for the matched parameters. In Section 4, we present the results of simulations that investigate the performance of our method in different settings. In Section 5, we discuss the findings from applying our method to the PROMPT mHealth trial. Finally, we conclude our paper in Section 6 with a brief summary.

2 Background and contributions

2.1 Gaussian graphical model

We start by briefly reviewing the GGM. Let X be a p dimensional random vector where

$$X = \left(X^{[1]}, X^{[2]}, \ldots, X^{[p]}\right) \sim N_p(0_p, \Sigma),$$

and Σ is an invertible $p \times p$ covariance matrix. Let $\Theta = \Sigma^{-1}$ be the precision matrix, with the $(j,k)^{\text{th}}$ element denoted by $\theta_{j,k}$.

Denote by $X^{[j]}$ the jth entry in the p dimensional Gaussian vector X. If $j \neq k \in \{1, 2, \ldots, p\}$, then $X^{[j]}$ and $X^{[k]}$ are independent conditional on the remaining entries in the random vector X if and only if $\theta_{jk} = \theta_{kj} = 0$. That is,

$$X^{[j]} \perp\!\!\!\perp X^{[k]} \Big| \left(X^{[l]}\right)_{l \neq j,k} \text{ if and only if } \theta_{jk} = \theta_{kj} = 0.$$

This fact implies that the support set $\text{Supp}(\Theta)$, excluding the diagonal entries, represents the edge structure of the graph.

Moreover, the $(j,k)^{\text{th}}$ entry of the precision matrix Θ is, up to a positive scalar, the regression coefficient of the kth variable in the multiple regression of jth variable on the rest, and vice-versa. This forms the basis of multiple regression, a popular framework for estimating the conditional dependence relationships in a GGM.

2.2 Selecting edges in the GGM

Suppose that we observe n independent realizations of X, which we denote by

$$X_1, X_2, \ldots, X_n,$$

and let $\mathbf{X}$ be the $n \times p$ matrix with $X_i \in \mathbb{R}^p$ in its ith row. Let $\mathbf{X}^{[-j]}$ represent the submatrix of $\mathbf{X}$ excluding the jth column and let $\mathbf{X}^{[j]}$ represent the jth column of $\mathbf{X}$.

Neighborhood selection, introduced by Meinshausen et al. (2006) computes a series of nodewise Lasso regressions by solving

$$\underset{b \in \mathbb{R}^{p-1}}{\text{minimize}} \ \ \frac{1}{2}\|\mathbf{X}^{[i]} - \mathbf{X}^{[-i]}b\|_2^2 + \lambda_i \|b\|_1 \tag{1}$$

for $i \in \{1, 2, \ldots, p\}$. Note, the regression at node i uses the ith variable as the response and the remaining variables as predictors.

The nodewise Lasso coefficients estimate the neighborhood for each of the p variables, and are combined to estimate $\text{Supp}(\Theta)$, which is equivalent to estimating the edge structure in the graph. For example, the $(j,k)^{\text{th}}$ entry of Θ is estimated to be non-zero using the "OR" logic if either the estimated Lasso coefficient of the jth variable on the kth variable or the estimated coefficient of the kth variable on the jth variable is non-zero. Alternatively, the "AND" logic can be used to combine the Lasso coefficients for estimating the graph. The nodewise regression approach taken by neighborhood selection has other important extensions, including a symmetric Lasso regression approach by Peng et al. (2009), as well as the estimation of more general network models beyond GGM (Ravikumar et al., 2010; Yang et al., 2015).

An alternative method for estimating a sparse precision matrix is the graphical lasso by Friedman et al. (2008). It uses the maximum likelihood approach to produce a matrix estimator of Θ, which can be solved through a block-wise coordinate descent algorithm. Al-

though this method is more computationally intensive than neighborhood selection, which solves p separable lasso regressions, it may be preferred in applications where an estimator for entries of the precision matrix is desired, rather than just a sparse support set for the edges. On the other hand, if the main goal of analysis is to estimate the sparse edge set, then neighborhood selection is usually easier to solve than graphical lasso. In addition, the nodewise Lasso regressions in neighborhood selection can be run in parallel on the data, making it substantially faster than graphical lasso. Finally, in many studies, measurements are of many different types (e.g., continuous, binary, counts). Recent work (Park et al., 2017; Yang et al., 2014) has extended graphical models to handle exponential family distributions in heterogeneous domains while permitting fast structure/parameter learning. While yet to be used extensively in practice, these methods provide psychologists with a useful tool for learning network models from heterogeneous data. The neighborhood selection algorithms we consider can be readily extended to this more general setting. This makes them a natural candidate as a starting point for selective inference for sparse Gaussian graphical models, as we consider the more general exponential family setting an important future direction.

2.3 Related work and our contributions

After conducting a series of Lasso regressions in equation (1), we obtain an estimate for the support of the precision matrix, denoted by $\text{Supp}(\widehat{\Theta})$. However, to obtain valid p-values or confidence bounds for the entries of Θ in the estimated support set using the same available data that was utilized in neighborhood selection, it is important to adjust for the selection of edges.

In Figure 1, "Naive" confidence intervals for the nonzero entries of the precision matrix,

in $\text{Supp}(\widehat{\Theta})$, are constructed for a range of values of $\lambda_i = \lambda$, $i \in \{1, 2, \ldots, p\}$ when data is generated from a GGM and nonzero edges are estimated using neighborhood selection. These intervals do not take into account the effect of selection. The mean coverage rate of the "Naive" intervals falls much below the target 90% rate, which highlights the pitfalls of not adjusting for the selection of edges.

An alternative approach is to use a subsample of the data for neighborhood selection and the remaining holdout samples that were not used for selection to construct intervals. This method, commonly referred to as "Data Splitting", is depicted in the same Figure. While "Data Splitting" provides valid selective inferences, it is wasteful since the resulting intervals are only based on the holdout dataset.

In this paper, we propose novel methodology that makes use of leftover information from selection to produce valid inferences for the selected entries in Θ. This method, which is presented in the next section, is referred to as "Proposed" in Figure 1. Our proposal not only achieves the prespecified coverage rate across the entire range of λ but also produces shorter intervals than data splitting. Both "Data Splitting" and "Proposed" generate longer intervals than "Naive", as they should, to account for the selection of edges. Below we discuss our key contributions and provide an overview of related work in selective inference.

Several methods have been proposed to address selective inference after Lasso regression. These include simultaneous methods by Berk et al. (2013b); Bachoc et al. (2020), conditional methods by Fithian et al. (2014); Lee et al. (2016a), and randomized conditional methods by Tian et al. (2018); Panigrahi and Taylor (2022); Rasines and Young (2022). The focus of this research is selective inference on the unknown mean parameter while treating the covariance of the response as a fixed parameter. The use of conditional meth-

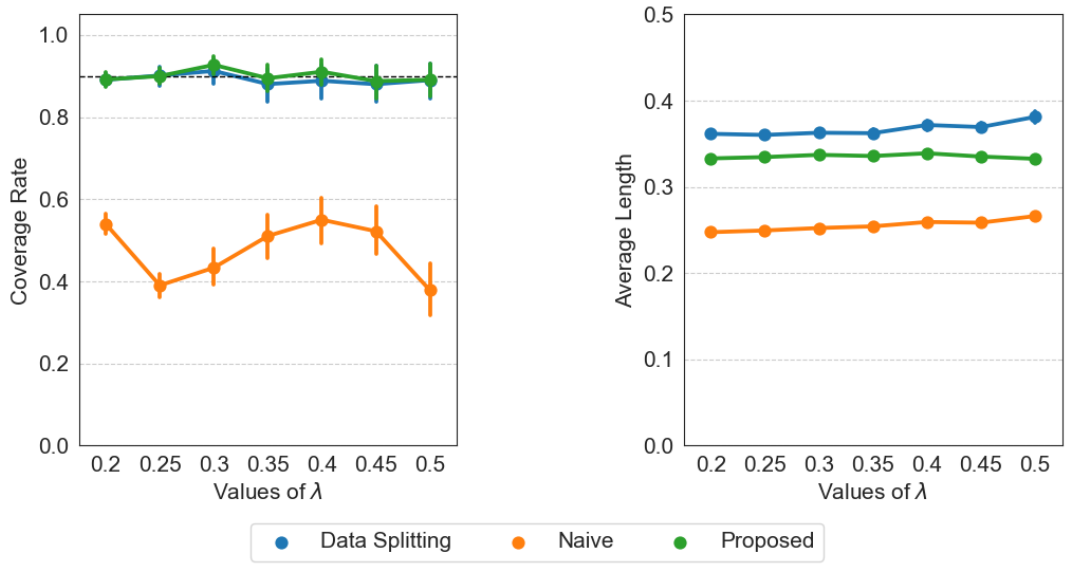

Figure 1: Coverage Rates and Average Confidence Interval Lengths of "Naive", "Data Splitting", and the Proposed Method for Gaussian Data with $n = 200$, $p = 10$ over 200 Simulations

ods in combination with externally added randomization adjusts for the specific selection via Lasso, producing bounded intervals and yielding more powerful inferences compared to those without randomization and conditioning. See, for example, results presented in recent papers by Kivaranovic and Leeb (2021); Panigrahi et al. (2021, 2022a). Whether or not randomization is applied, a key aspect of the conditional methods used for inference after Lasso regression is a neat polyhedral representation of the selection event. In the case of normal data, this means that the selection event can be expressed as a set of linear inequalities involving the normally distributed sufficient statistics, and the additional randomization variables if randomization is used.

Although neighborhood selection involves solving p separable Lasso regressions, selective inference in the GGM is not a simple extension of the method used for usual Lasso regression with normal data. This is because the selection event in terms of sufficient statistics in

the GGM, which follow a Wishart distribution, does not separate into individual nodewise regressions. Furthermore, this event no longer has a polyhedral representation in these sufficient statistics, which makes it even more challenging to provide selective inference for the selected edge parameters.

To tackle both challenges, we introduce a randomized conditional method that explicitly adjusts for selection via neighborhood selection in the GGM. Motivated by recent ideas of using randomization to account for non-polyhedral selection events, such as Panigrahi et al. (2022b, 2023); Huang et al. (2023), our method adds Gaussian randomization variables to the nodewise Lasso regressions in (1). We defer the specific form of Gaussian randomization used for our problem to the next section. Through the use of external randomization, we achieve two important goals. Firstly, we are able to describe the complex selection event as a set of simple sign constraints. Secondly, these constraints decouple across all the p regressions, allowing us to construct a pivot to infer for the selected entries in the precision matrix. The simplified selection event, facilitated by randomization, enables us to provide an efficient numerical algorithm for computing selective inferences in the GGM. The primary computing step of our algorithm can be performed in parallel across the nodewise regressions, similar to the selection step, which allows for fast inferences.

There have been recent proposals, such as those by Rasines and Young (2022) and Neufeld et al. (2023), suggesting alternative forms of randomization that differ from adding a randomization term to the regression objective. These methods can be used to create two randomized, independent copies of data for selection and inference, similar to data splitting, for normal data with a known covariance matrix. However, it is important to note that these methods do not provide a way to split the data into independent copies when the covariance is unknown, which is the case with the GGM. Our specific form of

randomization provides a way to carry over leftover information at the time of selecting the edges to drawing selective inferences.

3 Method

3.1 Randomized neighborhood selection

In this section, we present our randomized method for estimating the support set of Θ and addressing selective inferences for the estimated edges in the GGM. As emphasized earlier, the use of randomization is crucial for achieving feasible selective inferences in this problem.

We start with the randomized neighborhood selection method, which gives us the estimated support set for Θ. Consider p Gaussian randomization variables $w^{[i]}$ drawn from $N_{p-1}(0, \Omega^{[i]})$ for $i \in \{1, 2, \ldots, p\}$, where $w^{[i]}$ is independent of $\mathbf{X}$ and $w^{[i]}$ is independent of $w^{[j]}$ for all $i \neq j$. We solve p nodewise Lasso regressions as

$$\underset{b \in \mathbb{R}^{p-1}}{\text{minimize}} \quad \left\{ \frac{1}{2} \|\mathbf{X}^{[i]} - \mathbf{X}^{[-i]} b\|_2^2 + \lambda_i \|b\|_1 + \frac{\epsilon}{2} \|b\|_2^2 - b^\top w^{[i]} \right\}, \tag{2}$$

for each $i \in \{1, 2, \ldots, p\}$. The optimization problem is made strongly convex by including an additional ridge penalty with tuning parameter $\epsilon \in \mathbb{R}^+$. In our practical implementations of the method, we set the value of ϵ to a small positive value. The single regression problem with an added Gaussian randomization variable in the objective, described in Harris et al. (2016), is known as the randomized LASSO.

Adding a Gaussian randomization variable to each nodewise regression introduces a tradeoff between selection and inference, allowing us to reserve some information from the selection step to perform selective inference. During inference, our method conditions on the event of selection, which is based on the solution to the randomized neighborhood

selection. This allows us to adjust for the selection of edges while using leftover information from data used during this step. Note that our method differs from data splitting, which only uses holdout data for inference. Figure 1 confirms the expected gain in power over data splitting, providing a preview of our method's performance.

The solution of (2) leads us to observe

$$E_i \subset (\{1, 2, \ldots, p\} \setminus \{i\}),$$

the nonzero entries of the Lasso coefficients from the ith regression. Put another way, the set E_i gives us the estimated neighborhood for the ith variable. We define q_i as the number of non-zero entries in E_i, $\bar{E}_i$ as the complement set of $E_i \cup \{i\}$ and $\bar{q}_i$ as the size of $\bar{E}_i$, i.e., $|E_i| = q_i$, $\bar{E}_i = (E_i \cup \{i\})^c$, and $|\bar{E}_i| = p - 1 - q_i = \bar{q}_i$.

By combining the estimated neighborhoods of the p nodes using either the "AND" or "OR" rule, we obtain an estimate for the support of the precision matrix. In our next step, we present our method for drawing selective inference for $\theta_{j,k}$ whenever (j, k) is an entry in this estimated support set. However, before we delve into selective inference in the GGM, we fix some basic notations to warm up.

3.2 Some basics

Let M be a matrix in $\mathbb{R}^{p \times q}$ and let A and B be subsets of $\{1, 2, \ldots, p\}$ and $\{1, 2, \ldots, q\}$, respectively. We denote the submatrix of M with rows from A and columns from B as $M_{A,B}$. Moreover, we denote the submatrix of M with columns from B as M_B. Similarly, if V is a vector in $\mathbb{R}^p$, we denote the subvector of V with components from A as V_A. We use $I_{m,m}$ to represent the identity matrix of dimension m, $0_{p,q} \in \mathbb{R}^{p \times q}$ to represent the zero matrix of dimensions $p \times q$, and $0_q \in \mathbb{R}^q$ to represent the zero vector of dimension q. Throughout, we use the symbol $\phi(x; \mu, \Sigma)$ to represent the density at x of a multivariate

Gaussian distribution with mean μ and covariance matrix Σ. We use $f_\Theta(s)$ for the Wishart density at $s \in \mathbb{R}^{p\times p}$, which is given by

$$f_\Theta(s) \propto (\det s)^{(n-p-1)/2} \exp\left(-\frac{1}{2}\operatorname{tr}(\Theta s)\right) \cdot \mathbf{1}_{\mathbb{S}_+^p}(s),$$

where $\mathbb{S}_+^p$ is the cone of p-dimensional positive definite matrices.

We start by simplifying some of our notations. To this end, we assume $\lambda_i = \lambda$ for $i \in \{1, 2, \ldots, p\}$. For this purpose, we assume that $\lambda_i = \lambda$ for every i in the set $\{1, 2, \ldots, p\}$. Note that our method for selective inference can easily be generalized even when we have p distinct tuning parameters. Additionally, we assume without a loss of generality that the predictor matrix and randomization variable in each regression are reordered to have the components in E_i stacked above the components in $\bar{E}_i$.

We define some more estimators besides the selected set of edges E_i for $i \in \{1, 2, \ldots, p\}$, which will be needed for constructing selective inferences. Denote by

$$\begin{pmatrix} S_\lambda^{[i]} \\ Z_\lambda^{[i]} \end{pmatrix} = \partial \|b\|_1 \Big|_{B_\lambda^{[i]}},$$

the subgradient of Lasso penalty at the solution of the ith regression, where

$$S_\lambda^{[i]} = \operatorname{sign}\left(B_\lambda^{[i]}\right) \text{ and } \left\|Z_\lambda^{[i]}\right\|_\infty \leq 1.$$

Let $S = \mathbf{X}^\top \mathbf{X}$, with support equal to $\mathbb{S}_+^p$. We represent the $(j,k)^{\text{th}}$ entry of S as $S_{j,k}$. The value of $S_{j,k}$ is calculated by taking the dot product of the jth and k^{th} columns of $\mathbf{X}$. In the rest of the paper, we use s to denote the realized value of S and $s_{i,j}$ to denote the realized value of its $(j,k)^{\text{th}}$ entry.

Using these notations, let

$$T^{[i]} = -s_{-i,i},\ U^{[i]} = \begin{bmatrix} s_{E_i,E_i} + \epsilon I_{q_i,q_i} & 0_{q_i,\bar{q}_i} \\ s_{\bar{E}_i,E_i} & \lambda I_{\bar{q}_i,\bar{q}_i} \end{bmatrix},\ V^{[i]} = \lambda \begin{pmatrix} s_\lambda^{[i]} \\ 0_{\bar{q}_i} \end{pmatrix}.$$

For fixed s, define the mapping $\Pi_s^{[i]} : \mathbb{R}^{p-1} \to \mathbb{R}^{p-1}$ as

$$\Pi_s^{[i]}(b, z) = T^{[i]} + U^{[i]} \begin{pmatrix} b \\ z \end{pmatrix} + V^{[i]}, \tag{3}$$

where $b \in \mathbb{R}^{q_i}$ and $z \in \mathbb{R}^{\bar{q}_i}$, and define its inverse function as

$$\Delta_s^{[i]} = \left(\Pi_s^{[i]}\right)^{-1}.$$

Let $\mathcal{H}^{[i]} = \left\{b : \mathrm{Sgn}(b) = s_\lambda^{[i]}\right\}$ and $\mathcal{K}^{[i]} = \left\{z : \|z\|_\infty \leq 1\right\}$. Then, we note that

$$\begin{aligned} w^{[i]} &= -s_{-i,i} + \begin{bmatrix} s_{E_i,E_i} + \epsilon I_{q_i,q_i} & 0_{q_i,\bar{q}_i} \\ s_{\bar{E}_i,E_i} & \lambda I_{\bar{q}_i,\bar{q}_i} \end{bmatrix} \begin{pmatrix} b_\lambda^{[i]} \\ z_\lambda^{[i]} \end{pmatrix} + \lambda \begin{pmatrix} s_\lambda^{[i]} \\ 0_{\bar{q}_i} \end{pmatrix} \\ &= T^{[i]} + U^{[i]} \begin{pmatrix} b_\lambda^{[i]} \\ z_\lambda^{[i]} \end{pmatrix} + V^{[i]} \\ &= \Pi_s^{[i]}\left(b_\lambda^{[i]}, z_\lambda^{[i]}\right), \end{aligned} \tag{4}$$

where

$$b_\lambda^{[i]} \in \mathcal{H}^{[i]} \text{ and } z_\lambda^{[i]} \in \mathcal{K}^{[i]}.$$

Finally, we specify some of our general notation rules. We use lowercase letters to represent variable realizations in our data. For example, the observed realizations for the random variables $W^{[i]}$, $B_\lambda^{[i]}$, $S_\lambda^{[i]}$, $Z_\lambda^{[i]}$ are denoted by $w^{[i]}$, $b_\lambda^{[i]}$, $s_\lambda^{[i]}$, $z_\lambda^{[i]}$, respectively. Furthermore, we use uppercase bold font letters to denote collections of random variables that are collected for the p nodewise regressions, and lowercase bold font letters to denote their corresponding realized values. For example, we use $\mathbf{W} = \left\{W^{[i]}\right\}_{i=1}^p$, $\mathbf{B}_\lambda = \left\{B_\lambda^{[i]}\right\}_{i=1}^p$, $\mathbf{S}_\lambda = \left\{S_\lambda^{[i]}\right\}_{i=1}^p$, $\mathbf{Z}_\lambda = \left\{Z_\lambda^{[i]}\right\}_{i=1}^p$ to represent collections of the variables $W^{[i]}$, $B_\lambda^{[i]}$, $S_\lambda^{[i]}$, $Z_\lambda^{[i]}$ for $i \in \{1, 2, \ldots, p\}$, and we use $\mathbf{w} = \left\{w^{[i]}\right\}_{i=1}^p$, $\mathbf{b}_\lambda = \left\{b_\lambda^{[i]}\right\}_{i=1}^p$, $\mathbf{s}_\lambda = \left\{s_\lambda^{[i]}\right\}_{i=1}^p$, $\mathbf{z}_\lambda = \left\{z_\lambda^{[i]}\right\}_{i=1}^p$ for their respective realizations.

We are ready to construct inferences for the selected edges in the estimated support of Θ.

3.3 An exact adjustment for the selection of edges

In this section, our main result in Proposition 3.2 provides an adjustment for the selection of edges in the GGM, based on the solution to (2). This adjustment, when multiplied with the Wishart density of the random matrix S, gives us the starting point to derive pivots for selective inferences.

We note that

$$\left\{\mathbf{E} = E, \mathbf{S}_\lambda = \mathbf{s}_\lambda\right\} = \left\{b_\lambda^{[i]} \in \mathcal{H}^{[i]}, z_\lambda^{[i]} \in \mathcal{K}^{[i]} \text{ for } i \in [p]\right\}, \tag{5}$$

which is a direct result of the well-studied Lasso penalty. To obtain an adjustment for the selection of edges, we first derive the joint distribution of $S, \mathbf{B}_\lambda, \mathbf{Z}_\lambda$ when conditioned on the above-stated selection event. We present Proposition 3.1, which leads to our main result in the section.

Proposition 3.1. *Consider the event*

$$\mathcal{C}_0 = \left\{\mathbf{E} = E, \mathbf{S}_\lambda = \mathbf{s}_\lambda\right\},$$

and let

$$D = \int f_\Theta(\widetilde{s}) \cdot \prod_{i=1}^{p} \phi\left(\Pi_{\widetilde{s}}^{[i]}\left(\widetilde{b}_\lambda^{[i]}, \widetilde{z}_\lambda^{[i]}\right); 0_{p-1}, \Omega^{[i]}\right) \cdot \det\left(\widetilde{s}_{E_i,E_i} + \epsilon I_{q_i}\right)$$
$$\times \mathbf{1}_{\mathcal{H}^{[i]}}\left(\widetilde{b}_\lambda^{[i]}\right) \cdot \mathbf{1}_{\mathcal{K}^{[i]}}\left(\widetilde{z}_\lambda^{[i]}\right) d\widetilde{b}_\lambda^{[i]} d\widetilde{z}_\lambda^{[i]} d\widetilde{s}.$$

Conditional on the event $\mathcal{C}_0$, the density function of $S, \mathbf{B}_\lambda, \mathbf{Z}_\lambda$ at $(s, \mathbf{b}_\lambda, \mathbf{z}_\lambda)$ is equal to

$$f_{\Theta;\mathcal{C}_0}(s, \mathbf{b}_\lambda, \mathbf{z}_\lambda) = D^{-1} \cdot f_\Theta(s) \cdot \prod_{i=1}^{p} \left\{\phi\left(\Pi_s^{[i]}\left(b_\lambda^{[i]}, z_\lambda^{[i]}\right); 0_{p-1}, \Omega^{[i]}\right) \det\left(s_{E_i,E_i} + \epsilon I_{q_i}\right)\right.$$
$$\left.\times \mathbf{1}_{\mathcal{H}^{[i]}}\left(b_\lambda^{[i]}\right)) \cdot \mathbf{1}_{\mathcal{K}^{[i]}}\left(z_\lambda^{[i]}\right)\right\}.$$

Proof. Observe that the joint density of the randomization variables given $S = s$ is

$$f_{\mathbf{W}|S}\left(w^{[1]}, \ldots, w^{[p]} \mid s\right) = \prod_{i=1}^{p} \phi\left(w^{[i]}; 0_{p-1}, \Omega^{[i]}\right).$$

For fixed s, applying the change of variables

$$W^{[i]} \overset{\Delta_s^{[i]}}{\mapsto} \left(B_\lambda^{[i]}, Z_\lambda^{[i]}\right),$$

for each $i \in [p]$, gives us

$$f_{\mathbf{B}_\lambda,\mathbf{Z}_\lambda|S}(\mathbf{b}_\lambda, \mathbf{z}_\lambda \mid s) \propto \prod_{i=1}^{p} \left(\det D_{\Pi_s^{[i]}}\left(b_\lambda^{[i]}, z_\lambda^{[i]}\right)\right) \cdot \phi\left(\Pi_s^{[i]}\left(b_\lambda^{[i]}, z_\lambda^{[i]}\right); 0_{p-1}, \Omega^{[i]}\right),$$

where $\det D_{\Pi_s^{[i]}}\left(b_\lambda^{[i]}, z_\lambda^{[i]}\right) = \lambda^{\bar{q}_i} \det\left(s_{E_i,E_i} + \epsilon I\right)$ is the Jacobian matrix associated with the mapping $\Pi_s^{[i]}$, computed in Lemma A.1.

Clearly, the joint density of $(S, \mathbf{B}_\lambda, \mathbf{Z}_\lambda)$ is equal to

$$f_{S,\mathbf{B}_\lambda,\mathbf{Z}_\lambda}(s, \mathbf{b}_\lambda, \mathbf{z}_\lambda) = f_\Theta(s) \cdot f_{\mathbf{B}_\lambda,\mathbf{Z}_\lambda|S}(\mathbf{b}_\lambda, \mathbf{z}_\lambda \mid s),$$

when combined with the marginal Wishart density of S. Because of the equivalence in (5), the density function of $(S, \mathbf{B}_\lambda, \mathbf{Z}_\lambda)$ conditional on $\mathcal{C}_0$ is given by

$$\begin{aligned} f_{\Theta;\mathcal{C}_0}(s, \mathbf{b}_\lambda, \mathbf{z}_\lambda) &\propto f_\Theta(s) \cdot f_{\mathbf{B}_\lambda,\mathbf{Z}_\lambda|S}(\mathbf{b}_\lambda, \mathbf{z}_\lambda \mid s) \cdot \mathbf{1}_{\mathcal{H}^{[i]}}\left(b_\lambda^{[i]}\right) \cdot \mathbf{1}_{\mathcal{K}^{[i]}}\left(z_\lambda^{[i]}\right) \\ &\propto f_\Theta(s) \prod_{i=1}^{p} \Big\{ \phi\left(\Pi_s^{[i]}\left(b_\lambda^{[i]}, z_\lambda^{[i]}\right); 0_{p-1}, \Omega^{[i]}\right) \det\left(s_{E_i,E_i} + \epsilon I_{q_i}\right) \\ &\qquad \times \mathbf{1}_{\mathcal{H}^{[i]}}\left(b_\lambda^{[i]}\right) \cdot \mathbf{1}_{\mathcal{K}^{[i]}}\left(z_\lambda^{[i]}\right) \Big\}. \end{aligned}$$

Normalizing this density proves our claim. □

Proposition 3.2. *Conditional on*

$$\mathcal{C} = \{\mathbf{E} = E, \mathbf{S}_\lambda = \mathbf{s}_\lambda, \mathbf{Z}_\lambda = \mathbf{z}_\lambda\}, \tag{6}$$

the density function of S at s, denoted by $f_{\Theta;\mathcal{C}}(s)$, is proportional to

$$f_\Theta(s) \cdot \prod_{i=1}^{p} \int_{\mathcal{H}^{[i]}} \phi\left(\Pi_s^{[i]}\left(\widetilde{b}_\lambda^{[i]}, z_\lambda^{[i]}\right); 0_{p-1}, \Omega^{[i]}\right) \cdot \det\left(s_{E_i,E_i} + \epsilon I_{q_i}\right) d\widetilde{b}_\lambda^{[i]}.$$

Proof. Starting from the joint density in Proposition 3.1, we condition further on $\mathbf{Z}_\lambda = \mathbf{z}_\lambda$. This gives us the density function of S, $\mathbf{B}_\lambda$ when conditioned on $\mathcal{C}$, which is proportional to

$$f_\Theta(s) \cdot \prod_{i=1}^{p} \phi\left(\Pi_s^{[i]}\left(b_\lambda^{[i]}, z_\lambda^{[i]}\right); 0_{p-1}, \Omega^{[i]}\right) \cdot \det\left(s_{E_i,E_i} + \epsilon I_{q_i}\right) \cdot \mathbf{1}_{\mathcal{H}^{[i]}}\left(b_\lambda^{[i]}\right).$$

Marginalizing over $B_\lambda^{[i]}$ results in the density of S given $\mathcal{C}$ and completes our proof. □

To sum up, Proposition 3.2 provides an exact adjustment to the Wishart distribution of S to account for the selection of edges in the GGM.

3.4 Pivot for selective inference

Using the adjusted density from the preceding section, we construct a pivot for each parameter $\theta_{j_0,k_0} \in \Theta^E$, which serves as the main object of selective inference.

To form this pivot, we derive a one-dimensional density function that only involves the parameter we are interested in, by conditioning further on the observed values of

$$\bar{S}_{j_0,k_0} = \{S_{j,k}, \quad \text{for all } (j,k) \neq (j_0,k_0)\}.$$

Theorem 3.3 states this density function, which leads us to our pivot by applying the probability integral transform based on the related cumulative distribution function (CDF).

We define some more notations to proceed. Let $\bar{s}_{j_0,k_0}$ denote the observed values of the variables $\bar{S}_{j_0,k_0}$. For $c \in \mathbb{R}$, we define

$$I_{j_0k_0}(c, \bar{s}_{j_0,k_0}) : \mathbb{R} \to \mathbb{R}^{p\times p}$$

where the $(j,k)^{\text{th}}$ entry of the matrix-valued mapping is given by

$$\left[I_{j_0k_0}(c, \bar{s}_{j_0,k_0})\right]_{j,k} = \begin{cases} c & \text{if } \ (j,k) = (j_0,k_0) \text{ or } \ (j,k) = (k_0,j_0) \\ s_{j,k} & \text{otherwise.} \end{cases}$$

Observe that $I_{j_0k_0}(c, \bar{s}_{j_0,k_0})$ simply replaces the $(j_0, k_0)^{\text{th}}$ and $(k_0, j_0)^{\text{th}}$ entry of the observed data matrix with c, while keeping all its other entries intact.

Recall that the matrices $T^{[i]}$ and $U^{[i]}$, which were defined in (4), can be viewed as mappings of the data matrix s. We let

$$T^{[i]}_{j_0k_0}(c, \bar{s}_{j_0,k_0}) = T^{[i]} \circ I_{j_0k_0}(c, \bar{s}_{j_0,k_0}),\ U^{[i]}_{j_0k_0}(c, \bar{s}_{j_0,k_0}) = U^{[i]} \circ I_{j_0k_0}(c, \bar{s}_{j_0,k_0}).$$

These notations specify how $T^{[i]}$ and $U^{[i]}$ depend on the $(j_0, k_0)^{\text{th}}$ entry of s. Define

$$\pi^{[i]}_{j_0k_0}(c, \bar{s}_{j_0,k_0}, b, z) = T^{[i]}_{j_0k_0}(c, \bar{s}_{j_0,k_0}) + U^{[i]}_{j_0k_0}(c, \bar{s}_{j_0,k_0}) \begin{pmatrix} b \\ z \end{pmatrix} + V^{[i]}. \tag{7}$$

Specifically, we can rewrite (4) as

$$w^{[i]} = \pi^{[i]}_{j_0k_0}(s_{j_0,k_0}, \bar{s}_{j_0,k_0}, b^{[i]}_\lambda, z^{[i]}_\lambda).$$

Theorem 3.3. *Define the sets*

$$\mathcal{G} = \{i \in [p] :\ j_0 \in E_i \wedge k_0 \in E_i\},\ \mathcal{F} = \{i \in [p] :\ j_0 \in E_i \vee k_0 \in E_i\}.$$

Let

$$\Lambda_{j_0,k_0}(c, \bar{s}_{j_0,k_0}) = \prod_{i \in \mathcal{F} \cup \{j_0,k_0\}} \int_{\mathcal{H}^i} \phi\left(\pi^{[i]}_{j_0k_0}(c, \bar{s}_{j_0,k_0}, \widetilde{b}^{[i]}_\lambda, z^{[i]}_\lambda); 0_{p-1}, \Omega^{[i]}\right) d\widetilde{b}^{[i]}_\lambda$$
$$\times \prod_{i \in \mathcal{G}} \det\left([I_{j_0k_0}(c, \bar{s}_{j_0,k_0})]_{E_i,E_i} + \epsilon I_{q_i}\right).$$

Then, the conditional density of S_{j_0,k_0} given the event in (6) *and $\bar{S}_{j_0,k_0} = \bar{s}_{j_0,k_0}$, at $c \in \mathbb{R}$, is given by*

$$\frac{(\det I_{j_0k_0}(c, \bar{s}_{j_0,k_0}))^{(n-p-1)/2} \exp(-\theta_{j_0k_0}c)\, \Lambda_{j_0,k_0}(c, \bar{s}_{j_0,k_0}) \cdot \mathbf{1}_{\mathbb{S}_+}(I_{j_0k_0}(c, \bar{s}_{j_0,k_0}))}{\int (\det I_{j_0k_0}(t, \bar{s}_{j_0,k_0}))^{(n-p-1)/2} \exp(-\theta_{j_0k_0}t)\, \Lambda_{j_0,k_0}(t, \bar{s}_{j_0,k_0}) \cdot \mathbf{1}_{\mathbb{S}_+}(I_{j_0k_0}(t, \bar{s}_{j_0,k_0}))dt}.$$

The previous result indicates that only a subset of the p regressions contribute to the univariate conditional density of S_{j_0,k_0}. This subset can be much smaller than p, especially

if the j_0^{th} node or the k_0^{th} node are significantly associated with a sparse subset of nodes in the graph. The simplification of the univariate density from the adjusted density of the random matrix S is explained in detail in the proof, which we defer to the Appendix.

Denote by $\mathbb{F}_{\mathcal{C};\bar{s}_{j_0,k_0}}(\cdot;\theta_{j_0,k_0})$ the CDF for this density. Corollary 3.3.1 presents our pivot, which we obtain after applying the probability integral transform to the CDF.

Corollary 3.3.1. *Conditional on*

$$\mathcal{C} = \left\{\mathbf{E} = E, \mathbf{S}_\lambda = \mathbf{s}_\lambda, \mathbf{Z}_\lambda = \mathbf{z}_\lambda, \bar{S}_{j_0,k_0} = \bar{s}_{j_0,k_0}\right\},$$

we have

$$\mathbb{F}_{\mathcal{C};\bar{s}_{j_0,k_0}}(S_{j_0,k_0};\theta_{j_0,k_0}) \sim \text{Uniform}(0,1).$$

3.5 Algorithm for computing selective inference

Finally, we offer an efficient algorithm to numerically compute selective inference using our pivot.

Instead of computing the integrals in our pivot, we use a constrained optimization problem to calculate them. This approach is based on a Laplace approximation, which was previously employed for selective inferences in Panigrahi et al. (2017, 2021). To put it formally, we have

$$\begin{aligned}
&\int_{\mathcal{H}^i} \phi\left(\pi_{j_0k_0}^{[i]}(c, \bar{s}_{j_0,k_0}, \widetilde{b}_\lambda^{[i]}, z_\lambda^{[i]}); 0_{p-1}, \Omega^{[i]}\right) d\widetilde{b}_\lambda^{[i]} \\
\approx &\exp\left(-\underset{\widetilde{b}_\lambda^{[i]} \in \mathcal{H}^{[i]}}{\text{minimize}} \frac{1}{2}\left(\pi_{j_0k_0}^{[i]}(c, \bar{s}_{j_0,k_0}, \widetilde{b}_\lambda^{[i]}, z_\lambda^{[i]})\right)^\top \left(\Omega^{[i]}\right)^{-1} \left(\pi_{j_0k_0}^{[i]}(c, \bar{s}_{j_0,k_0}, \widetilde{b}_\lambda^{[i]}, z_\lambda^{[i]})\right)\right).
\end{aligned}$$

In practice, we solve an unconstrained optimization problem through the use of a barrier

function

$$\mathrm{Bar}_{\mathcal{H}^i}\left(\widetilde{b}_\lambda^{[i]}\right) = \sum_{j\in[q_i]} \log\left(1 + \left(s_\lambda^{[i]} b^{[i]}\right)^{-1}\right).$$

Note that the barrier function enforces the sign constraints on our optimization variables by imposing a larger penalty as the variables move near the boundary of $\mathcal{H}^{[i]}$. That is, we solve

$$\begin{aligned} L_{j_0k_0}^{[i]}(c, \bar{s}_{j_0,k_0}) = \underset{\widetilde{b}_\lambda^{[i]}\in\mathbb{R}^{q_i}}{\text{minimize}} \Big\{ & \frac{1}{2}\left(\pi_{j_0k_0}^{[i]}(c, \bar{s}_{j_0,k_0}, \widetilde{b}_\lambda^{[i]}, z_\lambda^{[i]})\right)^\top \left(\Omega^{[i]}\right)^{-1} \left(\pi_{j_0k_0}^{[i]}(c, \bar{s}_{j_0,k_0}, \widetilde{b}_\lambda^{[i]}, z_\lambda^{[i]})\right) \\ & + \mathrm{Bar}_{\mathcal{H}^{[i]}}(\widetilde{b}_\lambda^{[i]})\Big\} \end{aligned} \tag{8}$$

for $i \in \mathcal{F} \cup \{j_0, k_0\}$.

Now, we are ready to compute our pivot by substituting $\Lambda_{j_0,k_0}(c, \bar{s}_{j_0,k_0})$ with

$$\widehat{\Lambda}_{j_0,k_0}(c, \bar{s}_{j_0,k_0}) = \prod_{i\in\mathcal{F}\cup\{j_0,k_0\}} \exp\left(-L_{j_0k_0}^{[i]}(c, \bar{s}_{j_0,k_0})\right) \cdot \prod_{i\in\mathcal{G}} \det\left([I_{j_0k_0}(c, \bar{s}_{j_0,k_0})]_{E_i,E_i} + \epsilon I_{q_i}\right) \tag{9}$$

in the conditional density in Theorem 3.3. Denote by

$$d(c, \bar{s}_{j_0,k_0}) = (\det I_{j_0k_0}(c, \bar{s}_{j_0,k_0}))^{(n-p-1)/2} \exp\left(-\theta_{j_0k_0} c\right) \widehat{\Lambda}_{j_0,k_0}(c, \bar{s}_{j_0,k_0}) \cdot \mathbf{1}_{\mathbb{S}_+}(I_{j_0k_0}(c, \bar{s}_{j_0,k_0})).$$

Then, the pivot we compute numerically is equal to

$$\widehat{\mathbb{F}}_{\mathcal{C};\bar{s}_{j_0,k_0}}(S_{j_0,k_0}; \theta_{j_0,k_0}) = \left(\sum_{t\in G} d(c, \bar{s}_{j_0,k_0})\right)^{-1} \cdot \sum_{t\in G: t\le S_{j_0,k_0}} d(c, \bar{s}_{j_0,k_0}). \tag{10}$$

Algorithm 1 provides the above-outlined steps to obtain our pivot.

Using our pivot, we compute two-sided p-values for the null hypothesis $H_0: \ \theta_{j_0,k_0} = \theta_0$ as

$$2\min\left(\widehat{\mathbb{F}}_{\mathcal{C};\bar{s}_{j_0,k_0}}(S_{j_0,k_0}; \theta_0), 1 - \widehat{\mathbb{F}}_{\mathcal{C};\bar{s}_{j_0,k_0}}(S_{j_0,k_0}; \theta_0)\right).$$

Inverting the test provides the $100(1-\alpha)\%$ confidence interval for θ_{j_0,k_0} as

$$\left\{\theta_0 \in \mathbb{R}: \quad \alpha/2 < \widehat{\mathbb{F}}_{\mathcal{C};\bar{s}_{j_0,k_0}}(S_{j_0,k_0}; \theta_0) < 1 - \alpha/2\right\}.$$

Algorithm 1 Numerically computing our pivot for $\theta_{j_0k_0}$

$G \leftarrow \{t_0, t_1, ..., t_M : t_i - t_{i-1} = \delta\}$, $\delta > 0$ ▷ Grid with M evenly spaced points with a distance of δ

for all c in grid G **do**

  for $i \in \mathcal{F} \cup \mathcal{G}$ **do**

    Store $\pi^{[i]}_{j_0k_0}(c, \bar{s}_{j_0,k_0}, b, z)$ in (7).

    if $i \in \mathcal{G}$ **then**

      Store $\det\left([I_{j_0k_0}(c, \bar{s}_{j_0,k_0})]_{E_i,E_i} + \epsilon I_{q_i}\right)$

    end if

    Solve $L^{[i]}_{j_0k_0}(c, \bar{s}_{j_0,k_0})$ in (8)

    Compute $\widehat{\Lambda}_{j_0,k_0}(c, \bar{s}_{j_0,k_0})$ in (9)

  end for

end for

Calculate $\widehat{\mathbb{F}}_{\mathcal{C};\bar{s}_{j_0,k_0}}(S_{j_0,k_0}; \theta_{j_0,k_0})$ as shown in (10) ▷ Pivot

  return $\widehat{\mathbb{F}}_{\mathcal{C};\bar{s}_{j_0,k_0}}(S_{j_0,k_0}; \theta_{j_0,k_0})$

At last, Lemma 3.4 notes that the above set is indeed an interval. This can be verified by showing that $\widehat{\mathbb{F}}_{\mathcal{C};\bar{s}_{j_0,k_0}}(S_{j_0,k_0}; \theta)$ is a monotone function in θ.

Lemma 3.4. *The function* $\widehat{\mathbb{F}}_{\mathcal{C};\bar{s}_{j_0,k_0}}(S_{j_0,k_0}; \theta_{j_0,k_0})$ *based on our numerical approximation in* (8) *is monotonically increasing in* θ_{j_0,k_0}.

We provide a proof for Lemma 3.4 in the Appendix, which is adapted from Lemma A.1 in Lee et al. (2016b).

Algorithm 2 outlines the steps to construct confidence intervals using our pivot.

Algorithm 2 Constructing confidence intervals for $\theta_{j_0 k_0}$

Require: Confidence level $\alpha \in (0, 1)$

$L \leftarrow \{\theta_0, \theta_1, ..., \theta_K : \theta_i - \theta_{i-1} = \delta\}$, $\delta > 0$ ▷ Grid with K evenly spaced points with a distance of δ

CI_List $\leftarrow \{\}$ ▷ Record $\theta \in L$ that are not rejected

for all θ in L **do**

  if $\widehat{\mathbb{F}}_{\mathcal{C};\bar{s}_{j_0,k_0}}(S_{j_0,k_0};\theta) \in (\alpha/2, 1-\alpha/2)$ **then**

    CI_List $\leftarrow$ CI_List $\cup \{\theta\}$

  end if

end for

$L_{(j_0,k_0)} \leftarrow$ min CI_List ▷ Lower confidence bound

$U_{(j_0,k_0)} \leftarrow$ max CI_List ▷ Upper confidence bound

return $\left(L_{(j_0,k_0)}, U_{(j_0,k_0)}\right)$

4 Simulation

4.1 Setup

In this section, we assess the performance of our method in providing selective inference for the estimated edges in the GGM and its potential in recovering the conditional dependence relationships in the related graph.

We generate our data from a multivariate Gaussian distribution with a sparse precision matrix. To do so, we closely follow the generative scheme described in Meinshausen et al. (2006).

First, we construct the symmetric, sparse precision matrix Θ. We introduce two parameters: $m \in \mathbb{N}$ and $c \in (0, 1)$. These parameters control the number of edges per node

(or equivalently the sparsity in the precision matrix) and the signal magnitude. Now, we consider the following steps.

1. Suppose that each covariate (node) X_i corresponds to a point $p_i \in \mathbb{R}^2$, where p_i's are independent and identically distributed samples from a 2-dimensional uniform distribution over the interval $[0,1] \times [0,1]$.

2. Two nodes X_i and X_j are connected ($\theta_{ij} = \theta_{ji} \neq 0$) at random with a probability of

$$\phi(d(i,j)/\sqrt{p}),$$

   where $d(i,j) = ||p_i - p_j||_2$, and ϕ is the standard Gaussian probability density function.

3. The edges are generated according to the probability in step 2, and edges are randomly removed until the graph satisfies the requirement that

$$\sum_{j \neq i} \mathbb{1}\{\theta_{ij} \neq 0\} \leq m.$$

4. For each i, $\theta_{ii} = 1$, and for connected nodes i, j, θ_{ij} is sampled randomly from a uniform distribution

$$\text{Unif}(0, c/m).$$

We set $\Sigma = \Theta^{-1}$ and sample $n = 400$ observations from a $p = 20$ dimensional multivariate Gaussian $N_p(\mathbf{0}, \Sigma)$.

To solve the problem of randomized neighborhood selection, we use the penalty weights

$$\lambda_i(\alpha) = \kappa_i \cdot 2\sqrt{n}\hat{\sigma}_i \bar{\Phi}^{-1}\left(\alpha/2p^2\right). \tag{11}$$

Here, α is a parameter that controls the probability of falsely including an edge in the estimated model. It is set at 0.1. $\bar{\Phi}$ is the survival function of the standard Gaussian distribution, and $\hat{\sigma}_i^2 = \frac{1}{n}(\mathbf{X}^{[i]})^\top \mathbf{X}^{[i]}$ is the sample variance for the ith covariate. The parameter

κ_i is a scalar value that can be tuned in experiments. This value of tuning parameter is taken from Meinshausen et al. (2006), where it was shown to recover the true sparse support of the precision matrix with probability with a high probability. Finally, to estimate the conditional dependence relationships in the graph, we consider both the "AND" and "OR" logic rules for combining the neighborhoods based on $\mathbf{E}$. Our method, which is depicted as "Proposed" throughout this section, is implemented with simple independent Gaussian randomization variables $w^{[i]} \sim N_{p-1}(0, I_{p-1,p-1})$ for $i \in \{1, 2, \ldots, p\}$.

4.2 Metrics

To summarize the performance of our method, we compute the following metrics.

Let $\widetilde{\mathbf{E}}$ denote the selected set of nonzero parameters after applying the "AND" and "OR" logic rules to combine the estimated neighborhoods based on $\mathbf{E}$. Let $\mathbf{E}_0$ denote the true sparse support of the precision matrix.

First, we compute the coverage rate of the confidence intervals $C_{\widetilde{\mathbf{E}},(j,k)}$ for θ_{jk} whenever $(j,k) \in \widetilde{\mathbf{E}}$:

$$\text{Coverage Rate} = \frac{\left|\left\{(j,k) \in \widetilde{\mathbf{E}} : \boldsymbol{\theta}_{jk} \in C_{\widetilde{\mathbf{E}},(j,k)}\right\}\right|}{|\widetilde{\mathbf{E}}|}$$

for each round of simulation. Next, we report the average length of the confidence intervals $C_{\widetilde{\mathbf{E}},(j,k)} = (L_{\widetilde{\mathbf{E}},(j,k)}, U_{\widetilde{\mathbf{E}},(j,k)})$:

$$\text{Average Length} = \frac{\sum_{(j,k)\in\widetilde{\mathbf{E}}} \left(U_{\widetilde{\mathbf{E}},(j,k)} - L_{\widetilde{\mathbf{E}},(j,k)}\right)}{|\widetilde{\mathbf{E}}|}.$$

To examine the accuracy in estimating the conditional dependence relationships in the graph, we compute F1 scores after conducting selective inferences. After selective inference, we decide which of the selected edges to include in the graph based on whether the confidence interval covers 0 or not. These edges are reported as statistically significant

discoveries by our method. The F1 score is the harmonic mean of precision and recall and is given by the formula:

$$\text{F1} = 2\frac{\text{Precision } \times \text{ Recall}}{\text{Precision } + \text{ Recall}}.$$

Here precision is equal to the proportion of the true edges among the the reported edges

$$\text{Precision } = \frac{\left|\mathbf{E}_0 \cap \left\{(j,k) \in \widetilde{\mathbf{E}} : 0 \notin C_{\widetilde{\mathbf{E}},(j,k)}\right\}\right|}{\left|\left\{(j,k) \in \widetilde{\mathbf{E}} : 0 \notin C_{\widetilde{\mathbf{E}},(j,k)}\right\}\right|},$$

while recall is defined as the proportion of the reported edges among the set of true edges

$$\text{Recall } = \frac{\left|\mathbf{E}_0 \cap \left\{(j,k) \in \widetilde{\mathbf{E}} : 0 \notin C_{\widetilde{\mathbf{E}},(j,k)}\right\}\right|}{|\mathbf{E}_0|}.$$

4.3 Baseline for comparison

We compare our inferential results to those obtained from a common benchmark method known as data splitting. This method involves dividing the data into two independent parts. In the selection step, half of our data samples are used to solve the neighborhood selection problem and estimate the edge structure in the graph. In the inference step, the remaining half of the data samples are reserved to form confidence intervals for the selected edge parameters in the GGM. Below, we provide a brief description of a pivot based on data splitting.

Borrowing similar notations as in the preceding section, let $S^{(1)}_{j,k}$ and

$$\bar{S}^{(1)}_{j,k} = \left\{S^{(1)}_{j',k'}, \quad \text{for all } (j',k') \neq (j,k)\right\}$$

denote the sufficient statistics in the standard Wishart density for $j \neq k$, but based on only 50% of the data samples. The superscript "(1)" distinguishes these statistics from the ones used in the last section, using the full data.

When inferring for $\theta_{j_0k_0}$ where the edge (j_0, k_0) is included in our graph from the selection step, we use the distribution of $S^{(1)}_{j_0,k_0}$. To obtain a pivot for the parameter of interest, we

condition on all other sufficient statistics, given by $\bar{S}^{(1)}_{j_0,k_0}$, in order to eliminate all nuisance parameters.

Note, with data splitting, the selected edges can be treated as fixed since inferences are conducted on a new independent dataset. To be precise, the density of $S^{(1)}_{j_0,k_0}$ given $\bar{S}^{(1)}_{j_0,k_0} = \bar{s}^{(1)}_{j_0,k_0}$, when evaluated at $c \in \mathbb{R}$, is given by

$$p_{\bar{s}_{j_0,k_0}}(c;\theta_{j_0k_0}) = \frac{\left(\det I_{j_0k_0}(c,\bar{s}^{(1)}_{j_0,k_0})\right)^{(n-p-1)/2} \exp\left(-\theta_{j_0k_0}c\right)\cdot \mathbf{1}_{\mathbb{S}^p_+}\left(I_{j_0k_0}(c,\bar{s}^{(1)}_{j_0,k_0})\right)}{\int \left(\det I_{j_0k_0}(t,\bar{s}^{(1)}_{j_0,k_0})\right)^{(n-p-1)/2} \exp\left(-\theta_{j_0k_0}t\right)\cdot \mathbf{1}_{\mathbb{S}^p_+}\left(I_{j_0k_0}(t,\bar{s}^{(1)}_{j_0,k_0})\right) dt}.$$

The derivation of this one-dimensional density follows directly from the Wishart density of

$$S^{(1)} = \{S^{(1)}_{j_0,k_0}\} \cup \bar{S}^{(1)}_{j_0,k_0},$$

after we condition on $\bar{S}^{(1)}_{j_0,k_0} = \bar{s}^{(1)}_{j_0,k_0}$. A pivot for θ_{j_0,k_0}, using data splitting, is obtained immediately by applying a probability integral transform to this density, which is equal to

$$\int_{-\infty}^{S^{(1)}_{j_0,k_0}} p_{\bar{s}_{j_0,k_0}}(c;\theta_{j_0k_0})\, ds \sim \text{Uniform}(0,1). \tag{12}$$

Inverting the pivot yields p-values and confidence intervals for our parameter in focus.

4.4 Findings

We summarize findings from 500 rounds of simulations in two main settings. In Setting I, we fix the graph connectivity parameter for each node as $m = 2$ and vary the signal magnitude parameter $c \in \{0.4, 0.5, 0.6, 0.7, 0.8\}$. In Setting II, we fix the signal magnitude parameter at $c = 1$ and vary the graph connectivity parameter $m \in \{1, 2, 3, 4, 5\}$. For both settings, we present a comparison between our method and the baseline method of data splitting using both the "AND" and "OR" rules to combine the selected neighborhoods.

The plots in Figure 2 and 3 display error bar plots for the inferential and accuracy metrics in Setting I. Similarly, the plots in Figure 4 and 5 show error bar plots for the

inferential and accuracy metrics in Setting II. Our method is depicted as "Proposed" in all of the plots.

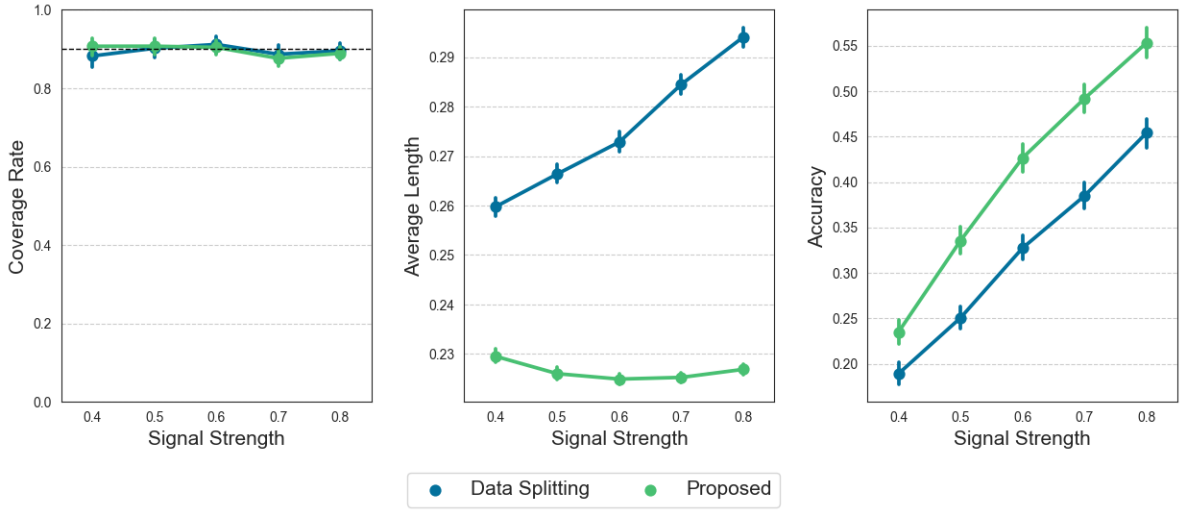

Figure 2: Coverage, length, and accuracy of selective inference for $m = 2$ and $c \in \{0.4, 0.5, 0.6, 0.7, 0.8\}$ using the "AND" rule.

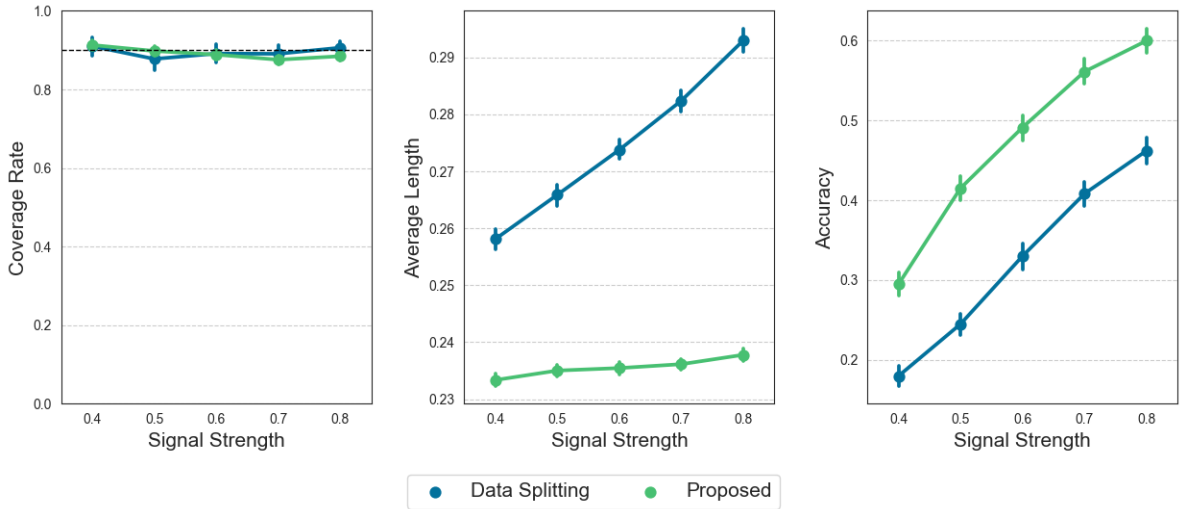

Figure 3: Coverage, length, and accuracy of selective inference for $m = 2$ and $c \in \{0.4, 0.5, 0.6, 0.7, 0.8\}$ using the "OR" rule.

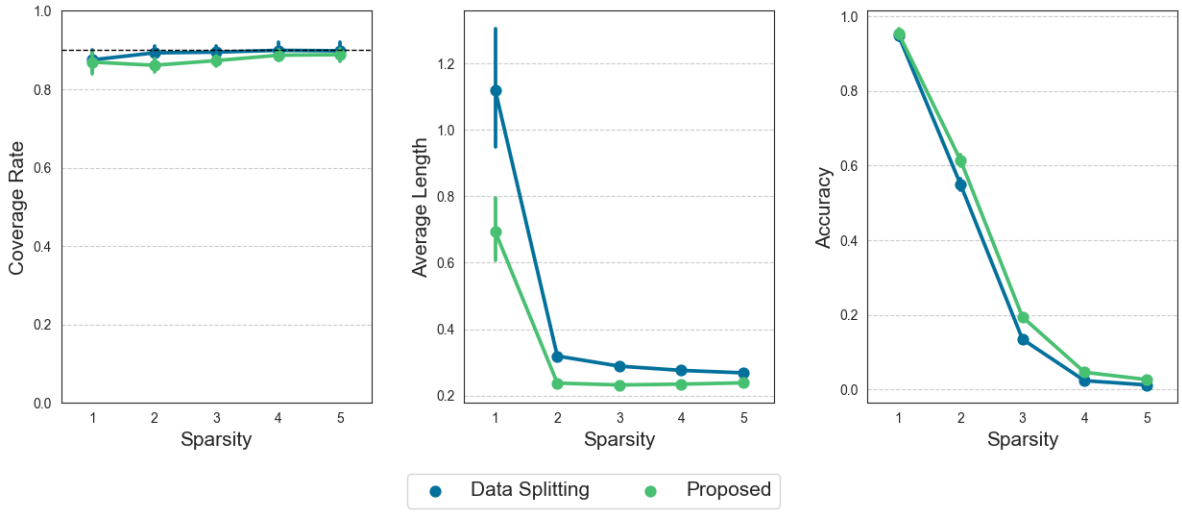

Figure 4: Coverage, length, and accuracy of selective inference for $c = 1$ and $m \in \{1, 2, 3, 4, 5\}$ using the "AND" rule.

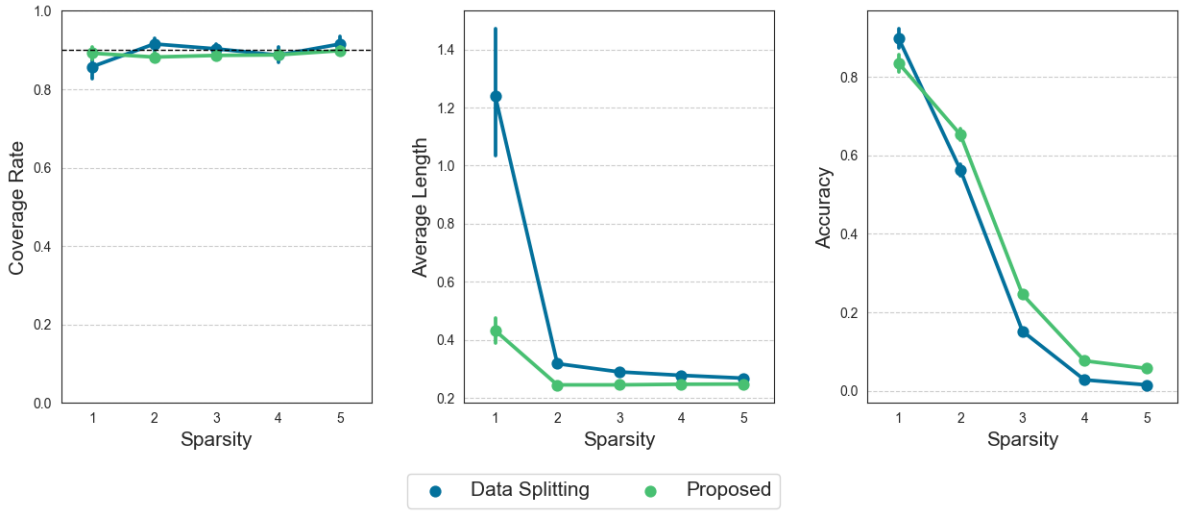

Figure 5: Coverage, length, and accuracy of selective inference for $c = 1$ and $m \in \{1, 2, 3, 4, 5\}$ using the "OR" rule.

For each setting, our simulations show that both "Proposed" and data splitting achieve the target coverage rate, which is set at 90%. However, our "Proposed" method produces narrower intervals than data splitting, indicating better inferential power. This is due to the use of leftover information from the selection step for inference. Moreover, our method

improves the accuracy of estimating the conditional dependence structure in the graph, which is measured by F1 scores. This shows that the "Proposed" method strikes a better balance between the amount of information used in selecting edges through neighborhood selection and the amount of information used exclusively for selective inference. All patterns for selective inference and estimation accuracy hold consistently for the "AND" and "OR" rules of combining estimated neighborhoods.

5 Case Study: PROMPT

Depression and anxiety, alongside sleep concerns and addiction, are rapidly escalating global health concerns, leading to increasing disability, lost productivity, and early deaths. Unfortunately, the current healthcare system, relying on traditional face-to-face therapy, is struggling to keep pace with the growing demand for mental health services. The *PROviding Mental health Precision Treatment (PROMPT) Precision Health Study* is a 12-month mobile health intervention trial focused on augmenting standard care to improve health outcomes by using mobile health technologies to extend the reach outside the clinic. Adult patients (age 18+) who have a scheduled adult mental health intake appointment at either Michigan Medicine Outpatient Psychiatry or University Health Service clinics were eligible for participation. Patients were required to have daily access to a smartphone in order to participate. Recruited patients entered study at least 2 weeks prior to their initial clinic appointment. Patients were randomized to (1) either receive or not receive enhanced feedback (EF) via the study app (e.g., on step count and heart rate goals) and (2) either have access to an additional mental health applicaiton (App) or not. Patients could not be randomized to receive neither EF nor the App, and therefore the study randomized to three conditions (EF + standard of care, App + standard of care, or EF + App + standard

of care). See here for additional details on the PROMPT study.

Participants were tasked with completing surveys throughout the study, including an initial intake survey, surveys at 6 weeks, 18 weeks, and 12 months into their participation. Participants were also notified via the study app on a daily basis to rate their mood on a scale of 1-10. After consenting to the study and completing the intake survey, each study participant received a free Fitbit to wear daily for the duration of their time in the study.

A key scientific aim of PROMPT is to better understand the complex relationships among treatment, baseline demographic information, survey responses, and mobile health signals. Here, we focus on the relationship among baseline survey instruments and wearable data collected via the Fitbit between 7 days prior to and 60 days after the baseline survey. This allows us to understand the relationship among these variables prior to the initial clinic visit. The intake survey included many standard, multi-item questionnaires such as the Patient Health Questionnaire (PHQ-9) and the General Anxiety Disorder (GAD-7). We pre-processed the intake survey to compute severity scores rather than analyzing individual items. Second, we summarized the 67 days of Fitbit data which consisted of 15 daily variables. As some Fitbit data streams require user input, there is a substantial amount of missing data in several data streams. We limit ourselves to datastreams with less than 20% missing data in each variable. The final list of variables is included in Table 3 from Appendix B. We then compute several summary statistics from the remaining daily wearable data such as means and standard deviations. Our final complete dataset consists of $N = 770$ patients with 9 survey variables, and 15 sensor variables.

Similar to our simulations in the preceding section, we solve the randomized neighborhood selection with standard Gaussian random variables. We set the tuning parameters in the nodewise multivariate regressions according to (11), where κ_i is set to 1. We ap-

plied the "OR" rule to combine the selected neighborhoods, resulting in the selection of 34 edges from a total of 276 possible edges. To construct selective inferences for these 34 edge parameters, we utilized Algorithm 2.

In Figure 6, we include a plot for the graph depicting the estimated conditional dependence relationships between the survey and sensor variables. The solid lines indicate edges which were significant post inference and the dotted lines indicate edges that were included in the graph at the selection step, but were no longer significant post inference. It is important to note that three of these edge parameters were deemed insignificant by our method, meaning that the confidence intervals returned for these parameters covered 0. This is accompanied by Tables 1 and 2, which report the confidence intervals formed through selective inference.

Our analysis suggests conditional independence between features from the wearable device and the baseline survey items. We can therefore conclude that there is not a strong relationship between various measures of physical activity and the severity scores among this population of treatment seeking individuals. We can thus analyze the wearable and baseline survey items separately. Among the features constructed from Fitbit data, we recover natural relationships such as the conditional dependence between distance and activity calories. Interestingly, calories was found to be conditionally independent of distance given activity calories suggesting that those calories burned during activity windows drives the overall distance covered by the individual. Among the baseline survey items, we recovered known relationships such as the GAD being conditionally dependent on PHQ and NEO, which measures neuroticism (N), extraversion (E), and openness (O). Interestingly, the Positive and Negative Suicide Ideation (PANSI) questionnaire was found to be conditionally independent of the GAD but dependent on the NEO and PHQ with the effect

seemingly larger for the PHQ. Most importantly, Tables 1 and 2 provide uncertainty quantification to ensure replication and reduce the risk of false discoveries from simply applying neighborhood selection to the observed mHealth data.

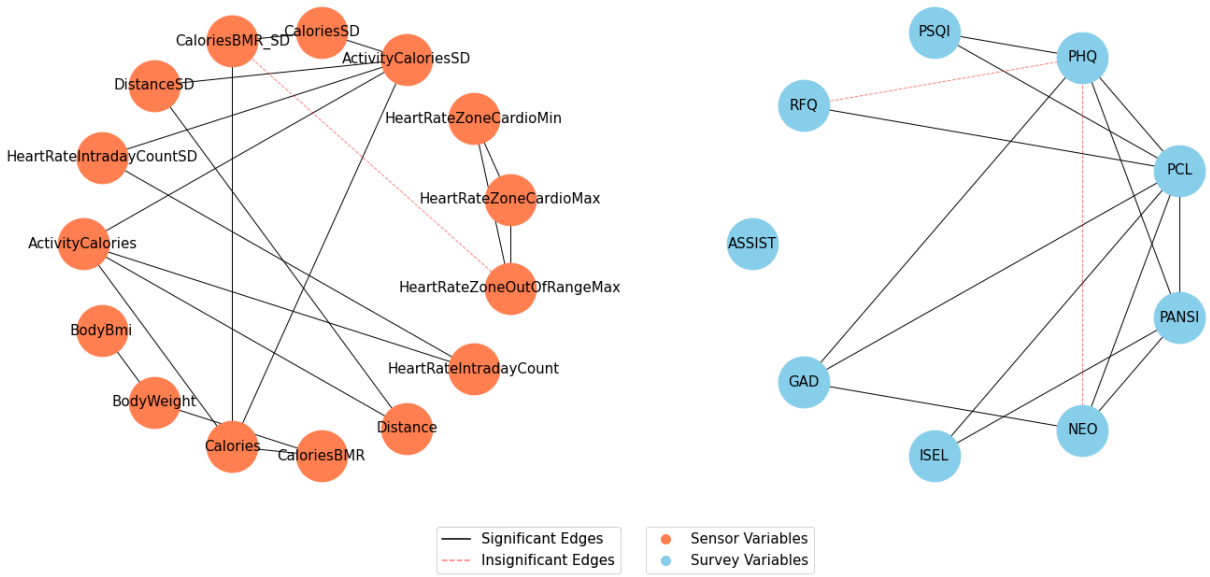

Figure 6: Visualization of graphs depicting the estimated conditional dependence relationships between the survey and sensor Variables

6 Conclusion

Precision health studies seek to understand the complex relationships among treatment, baseline demographic information, survey responses, and mobile health signals. This is achieved by learning the relevant conditional dependence relationships in a graphical model, which is equivalent to the presence or absence of an edge in the related graph. Although selecting edges and associating point estimates to the selected edges is prevalent, it can be misleading to report these edges without accompanying uncertainty estimates, given growing concerns about replicability.

	Activity Calories	Body Bmi	Body Weight	Calories	Calories BMR	Distance	HeartRate Intraday Count	HeartRate Zone OutOfRange Max	HeartRate Zone Cardio Max	HeartRate Zone Cardio Min	Activity Calories SD	Calories SD	Calories BMR_SD	Distance SD	HeartRate IntradayCount SD
ActivityCalories	-	-	-	(-87.47, -85.56)	-	(-25.94, -24.03)	(-2.89, -1.03)	-	-	-	(-36.25, -34.34)	-	-	-	-
BodyBmi	-	-	(-29.71, -27.80)	-	-	-	-	-	-	-	-	-	-	-	-
BodyWeight	-	-	-	-	(-50.65, -48.74)	-	-	-	-	-	-	-	-	-	-
Calories	-	-	-	-	(-97.05, -95.13)	-	-	-	-	-	(32.58, 34.49)	-	(36.30, 38.21)	-	-
CaloriesBMR	-	-	-	-	-	-	-	-	-	-	-	-	-	-	-
Distance	-	-	-	-	-	-	-	-	-	-	-	-	-	(-16.50, -14.59)	-
HeartRate IntradayCount	-	-	-	-	-	-	-	-	-	-	-	-	-	-	(-2.97, -2.39)
HeartRateZone OutOfRangeMax	-	-	-	-	-	-	-	-	(5.26, 6.89)	(-10.61, -8.82)	-	-	**(-1.09, 0.20)**	-	-
HeartRateZone CardioMax	-	-	-	-	-	-	-	-	-	(-50.20, -48.29)	-	-	-	-	-
HeartRateZone CardioMin	-	-	-	-	-	-	-	-	-	-	-	-	-	-	-
ActivityCaloriesSD	-	-	-	-	-	-	-	-	-	-	-	(-36.22, -34.31)	-	(-13.69, -11.78)	(-4.01, -2.80)
CaloriesSD	-	-	-	-	-	-	-	-	-	-	-	-	(-36.87, -34.95)	-	-
CaloriesBMR_SD	-	-	-	-	-	-	-	-	-	-	-	-	-	-	-
DistanceSD	-	-	-	-	-	-	-	-	-	-	-	-	-	-	-
HeartRate IntradayCountSD	-	-	-	-	-	-	-	-	-	-	-	-	-	-	-

Table 1: Confidence Intervals for Sensor Data

	ASSIST	GAD	ISEL	NEO	PANSI	PCL	PHQ	PSQI	RFQ
ASSIST	-	-	-	-	-	-	-	-	-
GAD	-	-	-	(-0.83, -0.54)	-	(-0.83, -0.51)	(-1.07, -0.73)	-	-
ISEL	-	-	-	-	(-0.36, -0.12)	(-0.33, -0.07)	-	-	-
NEO	-	-	-	-	(-0.48, -0.22)	(-0.30, -0.01)	**(-0.17, 0.13)**	-	-
PANSI	-	-	-	-	-	(-0.30, -0.01)	(-1.17, -0.86)	-	-
PCL	-	-	-	-	-	-	(-0.89, -0.54)	(-0.57, -0.30)	(-0.30, -0.04)
PHQ	-	-	-	-	-	-	-	(-0.34, -0.07)	**(-0.03, 0.25)**
PSQI	-	-	-	-	-	-	-	-	-
RFQ	-	-	-	-	-	-	-	-	-

Table 2: Confidence Intervals for Survey Data

In this paper, we propose a method for attaching uncertainties to the selected edges of undirected graphical models by using a selective inference approach. Our focus in the paper is on the widely used neighborhood selection method, which estimates the conditional dependence relationships in a graph through nodewise multivariate regressions. Unlike the usual single regression framework, the selection of edges does not have a simple polyhedral representation. However, by utilizing external randomization variables, our method provides an exact adjustment factor to account for the selection of edges. This exact adjustment takes the form of a few simple sign constraints, which decouple across the nodewise regressions.

To begin addressing selective inference in undirected graphical models, we considered inference on a single graph from Gaussian data. We believe that our current approach will pave the way for other crucial methods to tackle more general models and different types of data. For instance, this will involve extending the approach to a broader range of graphical models that encompass mixed data types, or performing integrative inferences for graphs that are aggregated across multiple time points or data sources. We leave these important extensions to future work.

References

Bachoc, F., Preinerstorfer, D., and Steinberger, L. (2020). Uniformly valid confidence intervals post-model-selection. *The Annals of Statistics*, 48:440–463.

Benjamini, Y. (2020). Selective inference: The silent killer of replicability. *Issue 2.4*, 2(4).

Benjamini, Y. and Yekutieli, D. (2005). False discovery rate–adjusted multiple confidence intervals for selected parameters. *Journal of the American Statistical Association*, 100(469):71–81.

Berk, R., Brown, L., Buja, A., Zhang, K., and Zhao, L. (2013a). Valid post-selection inference. *Annals of Statistics*, 41:802 – 837.

Berk, R., Brown, L., Buja, A., Zhang, K., and Zhao, L. (2013b). Valid post-selection inference. *The Annals of Statistics*, 41(2):802–837.

Borsboom, D., Fried, E., Epskamp, S., Waldorp, L., van Borkulo, C., van der Maas, H., and Cramer, A. (2017). False alarm? a comprehensive reanalysis of "evidence that psychopathology symptom networks have limited replicability" by forbes, wright, markon, and krueger (2017). *Journal of Abnormal Psychology*, 126:989–999.

Cramer, A., Borsboom, D., Aggen, S., and Kendler, K. (2012). The pathoplasticity of dysphoric episodes: differential impact of stressful life events on the pattern of depressive symptom inter-correlations. *Psychological Medicine*, 42:957–65.

Cramer, A., Waldorp, L., van der Maas, H., and Borsboom, D. (2010). Comorbidity: a network perspective. *Behavioral and Brain Sciences*, 33:137–50.

DeYoung, C. and Krueger, R. (2018). Understanding psychopathology: Cybernetics and psychology on the boundary between order and chaos. *Psychologial Inquiry*, 29:165–174.

Epskamp, S., Borsboom, D., and Fried, E. (2018a). Estimating psychological networks and their accuracy: A tutorial paper. *Behavior Research Methods*, 50:195–212.

Epskamp, S., Waldorp, L., Mottus, R., and Borsboom, D. (2018b). The gaussian graphical model in cross-sectional and time-series data. *Multivariate Behavioral Research*, 53:453–480.

Fithian, W., Sun, D., and Taylor, J. (2014). Optimal inference after model selection. *ArXiv.1410.2597*.

Forbes, M., Wright, A., Markon, K., and Krueger, R. (2019). Quantifying the reliability and replicability of psychopathology network characteristics. *Multivariate Behavioral Research*, pages 1–19.

Fried, E. and Cramer, A. (2017). Moving forward: Challenges and directions for psychopathological network theory and methodology. *Perspectives on Psychological Science*, 12:999–1020.

Friedman, J., Hastie, T., and Tibshirani, R. (2008). Sparse inverse covariance estimation with the graphical lasso. *Biostatistics*, 9(3):432–441.

Harris, X. T., Panigrahi, S., Markovic, J., Bi, N., and Taylor, J. (2016). Selective sampling after solving a convex problem. *arXiv preprint arXiv:1609.05609*.

Huang, Y., Pirenne, S., Panigrahi, S., and Claeskens, G. (2023). Selective inference using randomized group lasso estimators for general models. *arXiv preprint arXiv:2306.13829*.

Kivaranovic, D. and Leeb, H. (2021). On the length of post-model-selection confidence intervals conditional on polyhedral constraints. *Journal of the American Statistical Association*, 116(534):845–857.

Lee, J., Sun, D., Sun, Y., and Taylor, J. (2016a). Exact post-selection inference, with application to the lasso. *The Annals of Statistics*, 44(3):907–927.

Lee, J. D., Sun, D. L., Sun, Y., and Taylor, J. E. (2016b). Exact post-selection inference, with application to the lasso. *The Annals of Statistics*, 44(3):907–927.

Maxwell, S. E., Lau, M. Y., and Howard, G. S. (2015). Is psychology suffering from a replication crisis? what does "failure to replicate" really mean? *The American psychologist*, 70(6):487—498.

Meinshausen, N., Bühlmann, P., et al. (2006). High-dimensional graphs and variable selection with the lasso. *The annals of statistics*, 34(3):1436–1462.

Neufeld, A., Dharamshi, A., Gao, L. L., and Witten, D. (2023). Data thinning for convolution-closed distributions. *arXiv preprint arXiv:2301.07276*.

Panigrahi, S., Fry, K., and Taylor, J. (2022a). Exact selective inference with randomization. *arXiv preprint arXiv:2212.12940*.

Panigrahi, S., MacDonald, P. W., and Kessler, D. (2023). Approximate post-selective inference for regression with the group lasso. *Journal of Machine Learning Research*, 24(79):1–49.

Panigrahi, S., Markovic, J., and Taylor, J. (2017). An mcmc-free approach to post-selective inference. *arXiv preprint arXiv:1703.06154*.

Panigrahi, S., Stewart, N., Sripada, C. S., and Levina, E. (2022b). Selective inference for sparse multitask regression with applications in neuroimaging. *arXiv preprint arXiv:2205.14220*.

Panigrahi, S. and Taylor, J. (2022). Approximate selective inference via maximum likelihood. *Journal of the American Statistical Association*, pages 1–11.

Panigrahi, S., Zhu, J., and Sabatti, C. (2021). Selection-adjusted inference: an application to confidence intervals for cis-eqtl effect sizes. *Biostatistics*, 22(1):181–197.

Park, Y., Hallac, D., Boyd, S., and Leskovec, J. (2017). Learning the Network Structure of Heterogeneous Data via Pairwise Exponential Markov Random Fields. In Singh, A. and Zhu, J., editors, *Proceedings of the 20th International Conference on Artificial Intelligence and Statistics*, volume 54 of *Proceedings of Machine Learning Research*, pages 1302–1310, Fort Lauderdale, FL, USA. PMLR.

Peng, J., Wang, P., Zhou, N., and Zhu, J. (2009). Partial correlation estimation by joint sparse regression models. *Journal of the American Statistical Association*, 104(486):735–746.

Rasines, D. G. and Young, G. A. (2022). Splitting strategies for post-selection inference. *Biometrika*. to appear, asac070.

Ravikumar, P., Wainwright, M. J., and Lafferty, J. D. (2010). High-dimensional ising model selection using ℓ_1-regularized logistic regression. *The Annals of Statistics*, 38(3):1287–1319.

Tian, X., Taylor, J., et al. (2018). Selective inference with a randomized response. *The Annals of Statistics*, 46(2):679–710.

Yang, E., Baker, Y., Ravikumar, P., Allen, G., and Liu, Z. (2014). Mixed Graphical Models via Exponential Families. In Kaski, S. and Corander, J., editors, *Proceedings of the Sev-*

enteenth International Conference on Artificial Intelligence and Statistics, volume 33 of *Proceedings of Machine Learning Research*, pages 1042–1050, Reykjavik, Iceland. PMLR.

Yang, E., Ravikumar, P., Allen, G. I., and Liu, Z. (2015). Graphical models via univariate exponential family distributions. *The Journal of Machine Learning Research*, 16(1):3813–3847.

SUPPLEMENTARY MATERIAL

A Proofs of Results

We start with an auxiliary result that we use in the proof of Proposition 3.1 for constructing the selection-adjusted density of S:

Lemma A.1 (Jacobian of Change of Variable)**.** *Consider the mapping*

$$\Pi_s^{[i]}\left(B_\lambda^{[i]}, Z_\lambda^{[i]}\right) = T^{[i]} + U^{[i]}\begin{pmatrix} B_\lambda^{[i]} \\ Z_\lambda^{[i]} \end{pmatrix} + V^{[i]} = W^{[i]}.$$

Then, the Jacobian associated with $\Pi_s^{[i]}$ *when viewed as a change of variables mapping from* $W^{[i]}$ *to* $\left(B_\lambda^{[i]}, Z_\lambda^{[i]}\right)$ *is equal to*

$$\lambda_i^{\bar{q}_i} \det\left(s_{E_i,E_i} + \epsilon I_{q_i}\right).$$

Proof of Lemma A.1. Let $D_{\Pi_s^{[i]}}(B_\lambda^{[i]}, Z_\lambda^{[i]})$ be the differential of the map $\Pi_s^{[i]}$, given by

$$D_{\Pi_s^{[i]}}(B_\lambda^{[i]}, Z_\lambda^{[i]}) = \frac{\partial \Pi_s^{[i]}}{\partial\left(B_\lambda^{[i]}, Z_\lambda^{[i]}\right)}$$

Notice from the definition (4) that

$$\Pi_s^{[i]}\left(B_\lambda^{[i]}, Z_\lambda^{[i]}\right) = T^{[i]} + U^{[i]}\begin{pmatrix} B_\lambda^{[i]} \\ Z_\lambda^{[i]} \end{pmatrix} + V^{[i]}$$

and therefore

$$D_{\Pi_s^{[i]}}(B_\lambda^{[i]}, Z_\lambda^{[i]}) = \begin{pmatrix} \frac{\partial \Pi_s^{[i]}}{\partial B_\lambda^{[i]}} & \frac{\partial \Pi_s^{[i]}}{\partial Z_\lambda^{[i]}} \end{pmatrix} = \begin{pmatrix} (s_{E_i,E_i} + \epsilon I_{q_i}) & 0 \\ s_{\bar{E}_i,E_i} & \lambda_i I_{\bar{q}_i} \end{pmatrix}.$$

Noting that $D_{\Pi_s^{[i]}}(B_\lambda^{[i]}, Z_\lambda^{[i]})$ is a lower triangular matrix, we conclude that

$$\det D_{\Pi_s^{[i]}}(B_\lambda^{[i]}, Z_\lambda^{[i]}) = \det\left(s_{E_i,E_i} + \epsilon I_{q_i}\right)\det(\lambda_i I_{\bar{q}_i}) = \lambda_i^{\bar{q}_i}\det\left(s_{E_i,E_i} + \epsilon I_{q_i}\right).$$

□

Proof of Theorem 3.3. Observe that the conditional distribution of S has density proportional to

$$f_\Theta(s) \cdot \prod_{i=1}^{p} \int_{\mathcal{H}^{[i]}} \phi\left(\Pi_s^{[i]}\left(\widetilde{b}_\lambda^{[i]}, z_\lambda^{[i]}\right); 0_{p-1}, \Omega^{[i]}\right) \cdot \det\left(s_{E_i,E_i} + \epsilon I_{q_i}\right) d\widetilde{b}_\lambda^{[i]}$$

$$\propto (\det s)^{(n-p-1)/2} \cdot \exp\left(-\sum_{j,k\in[p]} \theta_{jk} s_{jk}\right) \cdot \mathbf{1}_{\mathbb{S}_+^p}(s)$$

$$\times \prod_{i=1}^{p} \int_{\mathcal{H}^{[i]}} \phi\left(\Pi_s^{[i]}\left(\widetilde{b}_\lambda^{[i]}, z_\lambda^{[i]}\right); 0_{p-1}, \Omega^{[i]}\right) \cdot \det\left(s_{E_i,E_i} + \epsilon I_{q_i}\right) d\widetilde{b}_\lambda^{[i]}.$$

If we condition further on $\{\bar{S}_{j_0,k_0} = \bar{s}_{j_0,k_0}\}$, then the conditional density of S_{j_0,k_0} at c is proportional to

$$(\det I_{j_0k_0}(c, \bar{s}_{j_0,k_0}))^{(n-p-1)/2} \exp\left(-\theta_{j_0k_0} c\right) \cdot \mathbf{1}_{\mathbb{S}_+^p}\left(I_{j_0k_0}(c, \bar{s}_{j_0,k_0})\right)$$

$$\times \prod_{i=1}^{p} \int_{\mathcal{H}^{[i]}} \phi\left(\pi_{j_0k_0}^{[i]}(c, \bar{s}_{j_0,k_0}, \widetilde{b}_\lambda^{[i]}, z_\lambda^{[i]}); 0_{p-1}, \Omega^{[i]}\right) \cdot \det\left(\left[I_{j_0k_0}(c, \bar{s}_{j_0,k_0})\right]_{E_i,E_i} + \epsilon I\right) d\widetilde{b}_\lambda^{[i]}.$$

The density in the above display follows from the definition of $I_{j_0k_0}(\cdot,\cdot)$ and the observation that conditional on $\bar{S}_{j_0,k_0} = \bar{s}_{j_0,k_0}$,

$$\Pi_{I_{j_0k_0}(c,\bar{s}_{j_0,k_0})}\left(b_\lambda^{[i]}, z_\lambda^{[i]}\right) = \pi_{j_0k_0}^{[i]}(c, \bar{s}_{j_0,k_0}, \widetilde{b}_\lambda^{[i]}, z_\lambda^{[i]})$$

for a fixed $c \in \mathbb{R}$. From the above-stated expression, we conclude that this conditional density is given by

$$\frac{(\det I_{j_0k_0}(c, \bar{s}_{j_0,k_0}))^{(n-p-1)/2} \exp\left(-\theta_{j_0k_0} c\right) \widetilde{\Lambda}_{j_0,k_0}(c, \bar{s}_{j_0,k_0}) \cdot \mathbf{1}_{\mathbb{S}_+}\left(I_{j_0k_0}(c, \bar{s}_{j_0,k_0})\right)}{\int (\det I_{j_0k_0}(t, \bar{s}_{j_0,k_0}))^{(n-p-1)/2} \exp\left(-\theta_{j_0k_0} t\right) \widetilde{\Lambda}_{j_0,k_0}(t, \bar{s}_{j_0,k_0}) \cdot \mathbf{1}_{\mathbb{S}_+}(I_{j_0k_0}(t, \bar{s}_{j_0,k_0})) dt},$$

where

$$\widetilde{\Lambda}_{j_0,k_0}(c, \bar{s}_{j_0,k_0}) = \left\{ \prod_{i=1}^{p} \det\left(\left[I_{j_0k_0}(c, \bar{s}_{j_0,k_0})\right]_{E_i,E_i} + \epsilon I\right) \right.$$

$$\left. \times \int_{\mathcal{H}^{[i]}} \phi\left(\pi_{j_0k_0}^{[i]}(c, \bar{s}_{j_0,k_0}, \widetilde{b}_\lambda^{[i]}, z_\lambda^{[i]}); 0_{p-1}, \Omega^{[i]}\right) d\widetilde{b}_\lambda^{[i]} \right\}.$$

In the remaining part of the proof, we derive a simplified expression for the conditional density of S_{j_0,k_0}. In order to obtain this expression, we observe that any term in

$\widetilde{\Lambda}_{j_0,k_0}(c, \bar{s}_{j_0,k_0})$ that does not depend on c will produce a constant factor in our density function.

We consider three cases for each $i \in [p]$, of which CASE II and CASE III, as defined later, give rise to an integral or a determinant term involved in $\widetilde{\Lambda}_{j_0,k_0}(c, \bar{s}_{j_0,k_0})$ that depend on c. We then derive a simplified expression for the conditional density of S_{j_0,k_0} using these terms.

CASE I. $\Big\{j_0 \notin E_i$ and $k_0 \notin E_i\Big\}$.

Note that in this case, the matrices $T^{[i]}$, $U^{[i]}$, and hence $\Pi_{I_{j_0k_0}(c,\bar{s}_{j_0,k_0})}\left(b_\lambda^{[i]}, z_\lambda^{[i]}\right)$ does not depend on $s_{j_0,k_0} = c$. Therefore, these terms can be disregarded from the conditional density.

CASE II. $\Big\{j_0 \in E_i$ and $k_0 \notin E_i\Big\}$ or $\Big\{j_0 \notin E_i$ and $k_0 \in E_i\Big\}$.

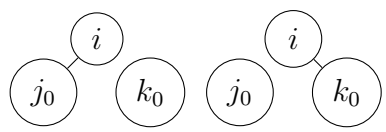

Figure 7: CASE II

An edge between i and j_0 or k_0 indicates $j_0 \in E_i$ or $k_0 \in E_i$, respectively

Recall that

$$\begin{aligned}
\pi_{j_0k_0}^{[i]}(c, \bar{s}_{j_0,k_0}, b, z) &= T_{j_0k_0}^{[i]}(c, \bar{s}_{j_0,k_0}) + U_{j_0k_0}^{[i]}(c, \bar{s}_{j_0,k_0}) \begin{pmatrix} b \\ z \end{pmatrix} + V^{[i]} \\
&= -\left[I_{j_0k_0}(c, \bar{s}_{j_0,k_0})\right]_{-i,i} + \begin{pmatrix} \left[I_{j_0k_0}(c, \bar{s}_{j_0,k_0})\right]_{E_i,E_i} + \epsilon I_{q_i,q_i} & 0_{q_i,\bar{q}_i} \\ \left[I_{j_0k_0}(c, \bar{s}_{j_0,k_0})\right]_{\bar{E}_i,E_i} & I_{\bar{q}_i,\bar{q}_i} \end{pmatrix} \begin{pmatrix} b \\ z \end{pmatrix} \\
&\quad + V^{[i]}.
\end{aligned}$$

First, suppose that $i \in [p] \setminus \{j_0, k_0\}$. Then, we note that $U^{[i]}_{j_0k_0}(c, \bar{s}_{j_0,k_0})$ depends on $s_{j_0,k_0} = c$, while $T^{[i]}_{j_0k_0}(c, \bar{s}_{j_0,k_0}) = [I_{j_0k_0}(c, \bar{s}_{j_0,k_0})]_{-i,i}$ does not depend on the value of s_{j_0,k_0}.

Next suppose that $i \in \{j_0, k_0\}$. In this case, $T^{[i]}_{j_0k_0}(c, \bar{s}_{j_0,k_0})$ depends on $s_{j_0,k_0} = c$, while $U^{[i]}_{j_0k_0}(c, \bar{s}_{j_0,k_0})$ does not depend on the value of s_{j_0,k_0}.

In both cases, the determinant

$$\det\left([I_{j_0k_0}(c, \bar{s}_{j_0,k_0})]_{E_i,E_i} + \epsilon I\right)$$

does not involve $s_{j_0,k_0} = c$, as E_i does not contain both j_0 and k_0 at the same time. To sum up, for any such i, the contribution to $\widetilde{\Lambda}_{j_0,k_0}(c, \bar{s}_{j_0,k_0})$ is equal to

$$\int_{\mathcal{H}^{[i]}} \phi\left(\pi^{[i]}_{j_0k_0}(c, \bar{s}_{j_0,k_0}, \widetilde{b}^{[i]}_\lambda, z^{[i]}_\lambda); 0_{p-1}, \Omega^{[i]}\right) d\widetilde{b}^{[i]}_\lambda.$$

CASE III. $\left\{j_0 \in E_i \text{ and } k_0 \in E_i\right\}$.

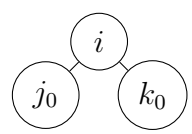

Figure 8: CASE III

Edges between i and j_0 and i and k_0 indicate $j_0 \in E_i$ and $k_0 \in E_i$.

It is easy to see that the term $U^{[i]}_{j_0k_0}(c, \bar{s}_{j_0,k_0})$ depends on $s_{j_0,k_0} = c$, and so does the determinant

$$\det\left([I_{j_0k_0}(c, \bar{s}_{j_0,k_0})]_{E_i,E_i} + \epsilon I\right).$$

Therefore, for each such i, the contribution to $\widetilde{\Lambda}_{j_0,k_0}(c, \bar{s}_{j_0,k_0})$ is equal to

$$\det\left([I_{j_0k_0}(c, \bar{s}_{j_0,k_0})]_{E_i,E_i} + \epsilon I\right) \times \int_{\mathcal{H}^{[i]}} \phi\left(\pi^{[i]}_{j_0k_0}(c, \bar{s}_{j_0,k_0}, \widetilde{b}^{[i]}_\lambda, z^{[i]}_\lambda); 0_{p-1}, \Omega^{[i]}\right) d\widetilde{b}^{[i]}_\lambda.$$

Combining the conclusions from the three possible cases leads us to note that $\widetilde{\Lambda}_{j_0,k_0}(c, \bar{s}_{j_0,k_0})$ can be replaced by $\Lambda_{j_0,k_0}(c, \bar{s}_{j_0,k_0})$, which completes the proof of the theorem. $\square$

Proof of Lemma 3.4. The conditional density that we numerically compute to obtain our pivot is equal to

$$\frac{(\det I_{j_0k_0}(S_{j_0k_0}, \bar{s}_{j_0,k_0}))^{(n-p-1)/2} \exp\left(-\theta_{j_0k_0} S_{j_0k_0}\right) \widehat{\Lambda}_{j_0,k_0}(S_{j_0k_0}, \bar{s}_{j_0,k_0}) \cdot \mathbf{1}_{\mathbb{S}_+}(I_{j_0k_0}(S_{j_0k_0}, \bar{s}_{j_0,k_0}))}{\int (\det I_{j_0k_0}(t, \bar{s}_{j_0,k_0}))^{(n-p-1)/2} \exp\left(-\theta_{j_0k_0} t\right) \widehat{\Lambda}_{j_0,k_0}(t, \bar{s}_{j_0,k_0}) \cdot \mathbf{1}_{\mathbb{S}_+}(I_{j_0k_0}(t, \bar{s}_{j_0,k_0}))dt}$$

when evaluated at $c = S_{j_0,k_0}$. Note that this density is an exponential family density:

$$p(S_{j_0k_0}; \eta) = \exp\left[\eta T(S_{j_0k_0}) - A(\eta)\right] h(S_{j_0k_0})$$

with the sufficient statistic $T(S_{j_0k_0}) = S_{j_0k_0}$ and the natural parameter $\eta = -\theta_{j_0k_0}$. Furthermore,

$$h(c) = \det I_{j_0k_0}(c, \bar{s}_{j_0,k_0}))^{(n-p-1)/2} \widehat{\Lambda}_{j_0,k_0}(c, \bar{s}_{j_0,k_0}) \cdot \mathbf{1}_{\mathbb{S}_+}(I_{j_0k_0}(c, \bar{s}_{j_0,k_0}),$$
$$A(-\theta_{j_0k_0}) = \log \int \exp\left(-\theta_{j_0k_0} t\right) h(t)dt.$$

Therefore, it admits a monotonic likelihood ratio, that is, for $\eta_0 = -\theta_0 < \eta_1 = -\theta_1$, the likelihood ratio $p(S_{j_0k_0}; \eta_1)/p(S_{j_0k_0}; \eta_0)$ is a monotonically increasing function in $S_{j_0k_0}$. This implies that for $c_1 > c_0$,

$$p(c_1; \eta_1)p(c_0; \eta_0) > p(c_0; \eta_1)p(c_1; \eta_0).$$

Now applying the proof of Lee et al. (2016b), we integrate over c_0 on $(-\infty, c)$, $c < c_1$ to obtain

$$\begin{aligned} p(c_1; \eta_1)\widehat{\mathbb{F}}_{\mathcal{C};\bar{s}_{j_0,k_0}}(c; \theta_0) &= \int_{-\infty}^{c} p(c_1; \eta_1)p(c_0; \eta_0)dc_0 \\ &> \int_{-\infty}^{c} p(c_0; \eta_1)p(c_1; \eta_0)dc_0 = p(c_1; \eta_0)\widehat{\mathbb{F}}_{\mathcal{C};\bar{s}_{j_0,k_0}}(c; \theta_1). \end{aligned}$$

Furthermore, integrating c_1 on (c, ∞) gives

$$\left(1 - \widehat{\mathbb{F}}_{\mathcal{C};\bar{s}_{j_0,k_0}}(c; \theta_1)\right) \widehat{\mathbb{F}}_{\mathcal{C};\bar{s}_{j_0,k_0}}(c; \theta_0) > \left(1 - \widehat{\mathbb{F}}_{\mathcal{C};\bar{s}_{j_0,k_0}}(c; \theta_0)\right) \widehat{\mathbb{F}}_{\mathcal{C};\bar{s}_{j_0,k_0}}(c; \theta_1),$$

and thus $\widehat{\mathbb{F}}_{\mathcal{C};\bar{s}_{j_0,k_0}}(c;\theta_0) > \widehat{\mathbb{F}}_{\mathcal{C};\bar{s}_{j_0,k_0}}(c;\theta_1)$ for $\theta_0 > \theta_1$. Hence $\widehat{\mathbb{F}}_{\mathcal{C};\bar{s}_{j_0,k_0}}(c;\theta)$ is monotonically increasing in θ. □

B PROMPT Variables

	Description
ActivityCalories	Calories burned from periods above sedentary level, personal average
BodyBmi	Body Mass Index, from the Body Time Series,
BodyWeight	Body weight, from the Body Time Series, personal average
Calories	Calories, from the Activity Time Series, personal average
CaloriesBMR	Only BMR (Basal Metabolic Rate) calories, from the Activity Time Series, personal average
Distance	Distance traveled, from the Activity Time Series, personal average
HeartRateIntradayCount	The number of intraday heart rate samples collected during the time period, personal average
HeartRateZoneOutOfRangeMax	The out of range max heart rate zone, personal average
HeartRateZoneCardioMax	The Cardio range max heart rate zone, personal average
HeartRateZoneCardioMin	The Cardio range min heart rate zone, personal average
ActivityCaloriesSD	Calories burned from periods above sedentary level, personal sd
CaloriesSD	Calories, from the Activity Time Series, personal average, personal sd
CaloriesBMR_SD	Only BMR (Basal Metabolic Rate) calories, from the Activity Time Series, personal sd
DistanceSD	Distance traveled, from the Activity Time Series, personal average, personal sd
HeartRateIntradayCountSD	The number of intraday heart rate samples collected during the time period, personal sd
ASSIST	The Alcohol, Smoking and Substance Involvement Screening Test score
GAD	General Anxiety Disorder Survey score
ISEL	Interpersonal Support Evaluation List score
NEO	NEO Personality Inventory score
PANSI	Positive and Negative Suicide Ideation score
PCL	PTSD Checklist score
PHQ	Patient Health Questionnaire score
PSQI	Pittsburgh Sleep Quality Index score
RFQ	The Reflective Functioning Questionnaire score

Table 3: Documentation for variables included in the PROMPT analysis